Evolution of immune genes in island birds: reduction in population sizes can explain island syndrome

Mathilde BARTHE[1*], Claire DOUTRELANT[2], Rita COVAS[3-5], Martim MELO[3-5], Juan Carlos ILLERA[6], Marie-Ka TILAK[1], Constance COLOMBIER[1], Thibault LEROY[1,7], Claire LOISEAU[2,3a], Benoit NABHOLZ[1,8a]

[1] ISEM, Univ Montpellier, CNRS, IRD, Montpellier, France

[2] Centre d'Ecologie Fonctionnelle et Evolutive, CNRS, Univ Montpellier, EPHE, IRD, Montpellier, France

[3] CIBIO, Research Centre in Biodiversity and Genetic Resources, InBIO Associated Laboratory, Campus Agrário de Vairão, Vairão, Portugal

[4] MHNC-UP, Natural History and Science Museum of the University of Porto, Porto, Portugal

[5] DST/NRF Centre of Excellence, FitzPatrick Institute, University of Cape Town, Rondebosch, South Africa

[6] Biodiversity Research Institute (CSIC-Oviedo University-Principality of Asturias), Oviedo University, Mieres, Spain

[7]IRHS-UMR1345, Université d'Angers, INRAE, Institut Agro, SFR 4207 QuaSaV, 49071, Beaucouzé, France

[8]Institut universitaire de France, Paris

[*] Corresponding author : mathilde.barthe.pro@gmail.com

[a] Last co-authors

Abstract

Shared ecological conditions encountered by species that colonize islands often lead to the evolution of convergent phenotypes, commonly referred to as ~~the~~ "island syndrome". Reduced immune functions have been previously proposed to be part of this syndrome, as a consequence of the reduced diversity of pathogens on island ecosystems. According to this hypothesis, immune genes are expected to exhibit genomic signatures of relaxed selection pressure in island species. In this study, we used comparative genomic methods to study immune genes in island species (N = 20) and their mainland relatives (N = 14). We gathered public data as well as generated new data on innate (TLR: Toll-Like Receptors, BD: Beta Defensins) and acquired immune genes (MHC: Major Histocompatibility Complex classes I and II), but also on hundreds of genes with various immune fonctions. As a control, we used a set of 97 genes, not known involved in immune functions based on the literature, to ~~account~~ the increased drift effects ~~for~~ the lower effective population sizes in island species. We used synonymous and non-synonymous ~~variations~~ to estimate the selection pressure acting on immune genes. BDs and TLRs have higher ratios of non-synonymous over synonymous polymorphisms (Pn/Ps) than randomly selected control genes suggesting that they evolve under a different selection regime ~~than non-immune related genes~~. However, simulations ~~analyses~~ show that this is unlikely to be explained by ongoing positive selection or balancing selection. For the MHC evolving under balancing selection, we used simulation to estimate the impact of population size variation. We found a significant effect of drift on immune genes of island species leading to a reduction in genetic diversity and efficacy of selection. However, the intensity of relaxed selection was not significantly different from control genes, except for MHC class II genes. These genes exhibit a significantly higher level of non-synonymous loss of polymorphism than expected assuming only drift and ~~an~~ evolution under frequency dependent selection, possibly due to a reduction of extracellular parasite communities on islands. Overall, our results showed that demographic effects lead to a decrease in the immune functions of island species, but the relaxed selection caused by a reduced parasite pressure may only occur in some ~~immune genes categories~~.

Keywords: genetic drift, island evolution, immunity, Toll-Like Receptors, Beta-Defensins, major histocompatibility complex, molecular evolution, population genomics

Introduction

Island colonizers face new communities of competitors, predators and parasites in a small area with limited resources, which generally result in high extinction rates of colonizers (Losos and Ricklefs, 2009). Oceanic island faunas are characterized by a low species richness, coupled with high population densities for each species (MacArthur and Wilson, 1967; Warren et al., 2015) - which translates in communities with, on average, low levels of inter-specific interaction and high levels of intra-specific competition (but see Rando et al., 2010 for an example of character displacement due to competition among island finch species). These shared island characteristics are thought to underlie the evolution of convergent phenotypes, in what is called the 'island syndrome' (Baeckens and Van Damme, 2020). Convergence has been documented in multiple traits, such as size modification (dwarfism or gigantism; Lomolino, 2005), reduction of dispersal (Baeckens and Van Damme, 2020) shift towards K life history strategies (Boyce, 1984; Covas, 2012; MacArthur and Wilson, 1967), evolution of generalist traits (Blondel, 2000; Warren et al., 2015), or changes in colour and acoustic signals (Doutrelant et al., 2016; Grant, 1965).

Reduced immune function has also been hypothesized as an island syndrome trait, directly linked to reduced parasite pressure on islands (Lobato et al., 2017; Matson and Beadell, 2010; Wikelski et al., 2004). Island parasite communities are i) less diverse (Beadell et al., 2006; Illera et al., 2015; Loiseau et al., 2017; Maria et al., 2009; Pérez-Rodríguez et al., 2013), and ii) could be less virulent due to the expansion of the ecological niche expected by the theory of island biogeography. In fact, island parasites are generally more generalists than their mainland counterparts, which could lead to a reduced virulence due to the trade-off between replication capacity and resistance against host immune defenses (Garamszegi, 2006; Hochberg and Møller, 2001; Pérez-Rodríguez et al., 2013). Overall, a reduction of parasitic pressure should lead to a weakening of the immune system due to the costs of maintaining efficient immune functions (Lindström et al., 2004; Matson and Beadell, 2010; Wikelski et al., 2004). Such reduction may have important implications for the ability of these populations to resist or tolerate novel pathogens. The introduction of avian malaria in the Hawaiian archipelago, and the subsequent extinctions and population declines of many endemic species is the most emblematic example (Van Riper III et al., 1986; Wikelski et al., 2004).

Immunological parameters, such as blood leukocyte concentration, antibodies or other immune proteins (e.g. haptoglobin), hemolysis, and hemagglutination (Lee et al., 2006; Matson and

Beadell, 2010) may serve as proxies to determine population immune functions. To date, the majority of studies that focused on island avifauna have found ambiguous results, with either no support for a reduced immune response on island species (Beadell et al., 2007; Matson, 2006), or ~~contrasted~~ results, such as a lower humoral component (total immunoglobulins) on islands, but a similar innate component (haptoglobin levels) between island and mainland species (Lobato et al., 2017). The use of immune parameters as proxies of immune function is fraught with difficulties (Lobato et al., 2017). The study of molecular evolution of immune genes therefore represents an alternative strategy to tackle this question. However, it is necessary to distinguish neutral effects, the demographic effects resulting from island colonization, from selective ones, the potential relaxation of selection pressures due to the changes in the pathogen community.

t, the bottleneck experienced by species during island colonization leads to a decrease in genetic variability (Frankham, 1997). A reduced genetic diversity at loci involved in immunity should have a direct implication on immune functions (Hale and Briskie, 2007 but see ; Hawley et al., 2005; Spurgin et al., 2011). Second, small population sizes increase genetic drift, which may counteract the effect of natural selection on weakly deleterious mutations (Ohta, 1992). Several recent studies found a greater load of deleterious mutations in island species (Kutschera et al., 2020; Leroy et al., 2021b; Loire et al., 2013; Robinson et al., 2016; Rogers and Slatkin, 2017). Finally, it is necessary to differentiate genes involved in the innate versus the acquired immune response. The innate immune response is the first line of defense and is composed of phagocytes, macrophages and dendritic cells. These cells allow non-specific recognition of pathogens (Akira, 2003; Alberts et al., 2002). For example, Toll-Like Receptors (TLR; transmembrane proteins) trigger a chain reaction leading to the production of various substances, including antimicrobial peptides such as beta-defensins (BD) that have active properties in pathogen cell lysis (Velová et al., 2018). On the other hand, the acquired immune system allows a specific response, characterized by immune memory. Major Histocompatibility Complex (MHC) genes code for surface glycoproteins that bind to antigenic peptides, and present them to the cells of the immune system; class I and II genes ensure the presentation of a broad spectrum of intra- and extracellular-derived peptides, respectively (Klein, 1986). Although all these genes are directly involved in the identification and neutralization of pathogens, previous studies found that they evolve under different selection regimes: TLRs and BDs are under purifying selection which usually results in the selective

removal of deleterious alleles and stabilizing selection (Grueber et al., 2014; van Dijk et al., 2008), whereas MHC genes are under balancing selection (Bernatchez and Landry, 2003).

Recent studies on birds (Gonzalez-Quevedo et al., 2015a, 2015b), amphibians (Belasen et al., 2019), and lizards (Santonastaso et al., 2017) found that the demographic history of island populations led to the loss of genetic variation at immune genes involved in pathogen recognition, such as TLRs and MHC. For example, (Santonastaso et al., 2017) demonstrated that the polymorphism pattern in MHC genes and microsatellites covary positively with island area in *Podarcis* lizards, suggesting a dominant role for genetic drift in driving the evolution of the MHC. Gonzalez-Quevedo, et al. (2015a) found a similar pattern comparing TLR and microsatellite polymorphism in the Berthelot pipit, *Anthus berthelotii*, an endemic species from Macaronesia, supporting a predominant role of genetic drift in TLR evolution. However, these studies did not explicitly test the hypothesis of a relaxed selection pressure on islands imposed by an impoverished parasite community. All other things being equal, it is expected that the polymorphism pattern of coding sequence decreases with population size (Buffalo, 2021; Leroy et al., 2021b). Therefore, a decrease in polymorphism with population size could not be taken as a proof of a relaxation in the selection pressure.

Here, we study a dataset of 34 bird species (20 insular and 14 mainland species; Figure 1) combining the 24 species of Leroy et al. (2021b) and 10 newly generated by targeted-capture sequencing (Table 1). To be able to demonstrate a change in natural selection, a traditional approach is to contrast polymorphism of synonymous sites (Ps) with polymorphism of non-synonymous sites (Pn). Synonymous mutations refer to mutations that do not alter amino acid sequences, whereas non-synonymous mutations do.

Following population genetic theory, in a diploid population, Ps = $4\ Ne\ \mu$ and Pn = $4\ Ne\ \mu\ f$, where Ne is the effective population size, μ is the mutation rate and f is a function that integrates the probability of an allele to segregate at a given frequency. f depends on the distribution of the fitness effect (DFE) of mutations (Eyre-Walker and Keightley, 2007). This distribution scales with Ne as the fitness effect is dependent on Ne multiplied by the coefficient of selection s (Kimura, 1962). The nearly-neutral theory predicts that the DFE includes a large proportion of mutations with a $Ne*s$ close to 0 (Ohta, 1992). As a consequence, an increase of Ne will lead to an increase of the fitness effect of weakly deleterious mutations, in such a way that these mutations will be more easily removed from the population by natural selection, therefore reducing Pn relative to Ps leading to a negative correlation between Pn/Ps and Ps (through Ne;

Welch et al., 2008). The presence of linked positively selected mutations does not change ~~qualitatively this relationship~~ (Castellano et al., 2018; Chen et al., 2020 and our simulations below).

Shifts in the parasitic community on islands are expected to have an impact on the rat[illegible]n/Ps of immune genes. However, the fixation probability depends on the product *Ne s*, and ~~a~~ variation in *Ne* is also expected to impact the efficacy of selection and thus the ratio Pn/Ps across the entire transcriptome, particularly in the presence of slightly deleterious mutations (Charlesworth and Eyre-Walker, 2008; Leroy et al., 2021b; Loire et al., 2013; Ohta, 1992). In addition, due to their lower population sizes, island birds compared to continental species exhibit a genome-wide reduction in genetic diversity and efficacy of selection (Kutschera et al., 2020; Leroy et al., 2021b). Therefore, we expect a similar reduction in immune gene~~s~~ diversity even without any change in the parasite pressure.

To disentangle the effect of population size from a change in parasite pressure and estimate the impact of demography on the efficacy of selection, we randomly selected protein-coding genes (i.e., control genes) involved in various biological functions (Fijarczyk et al., 2016; Leroy et al., 2021b). The selection pressure acting on the randomly selected control genes is expected to be similar between island and mainland bird species. Therefore, the variation of Pn/Ps of the control genes is only dependent on the variation of *Ne*. In contrast, if a reduced parasite pressure on islands directly impacts the evolution of immune genes, the Pn/Ps of immune genes is expected to show a larger variation between island and continental species than the control genes. More specifically, for genes under purifying selection, non-synonymous weakly deleterious mutations, normally eliminated under strong selection, would be maintained, leading to an increase of Pn/Ps. By contrast, for genes under balancing selection, non-synonymous advantageous mutations, normally maintained in the polymorphism under strong selection, would be fixed or eliminated leading to a decrease of Pn/Ps (Figure 2).

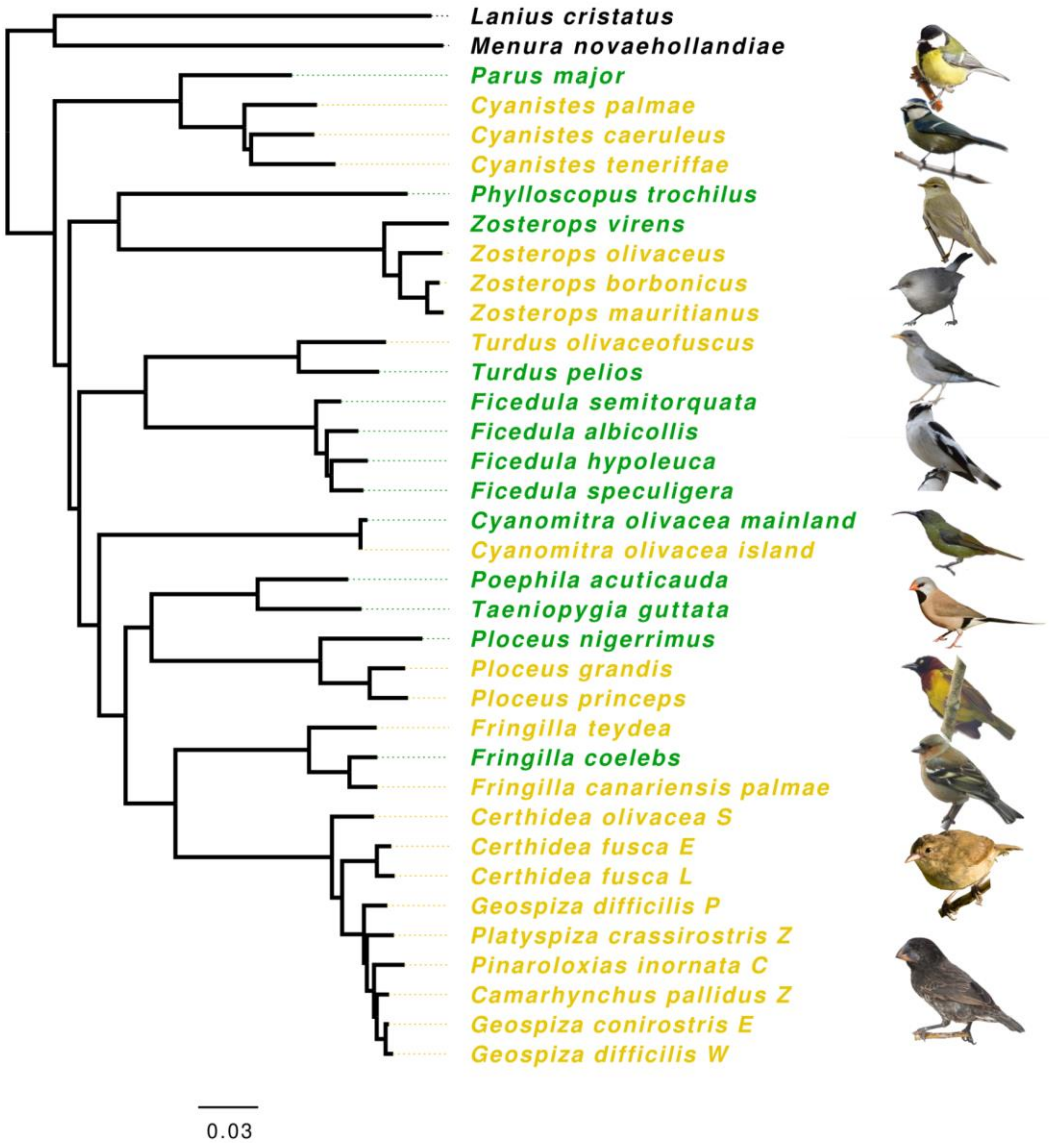

Figure 1: Phylogeny based on mitochondrial genes of species from the dataset reconstructed by maximum likelihood method (IQTREE model GTR+Gamma). Species names in yellow indicate island species, and in green, mainland species. Ultrafast bootstrap values are provided in the supplementary methods. Some relationships are poorly supported. Bird representations are not to scale. Photos from top to bottom : *P. major, C. caeruleus, P. trochilus, Z. borbonicus, T. pelios, F. albicollis, C. olivacea, P. acuticauda, P. grandis, F. coelebs, C. fusca, G. conirostris*. Photo credits: A. Chudý, F. Desmoulins, E. Giacone, G. Lasley, Lianaj, Y. Lyubchenko, B. Nabholz, J.D. Reynolds, K. Samodurov, A. Sarkisyan, Wimvz, Birdpics, T. Aronson, G. Lasley, P. Vos (iNaturalist.org); M. Gabrielli (*Zosterops borbonicus*).

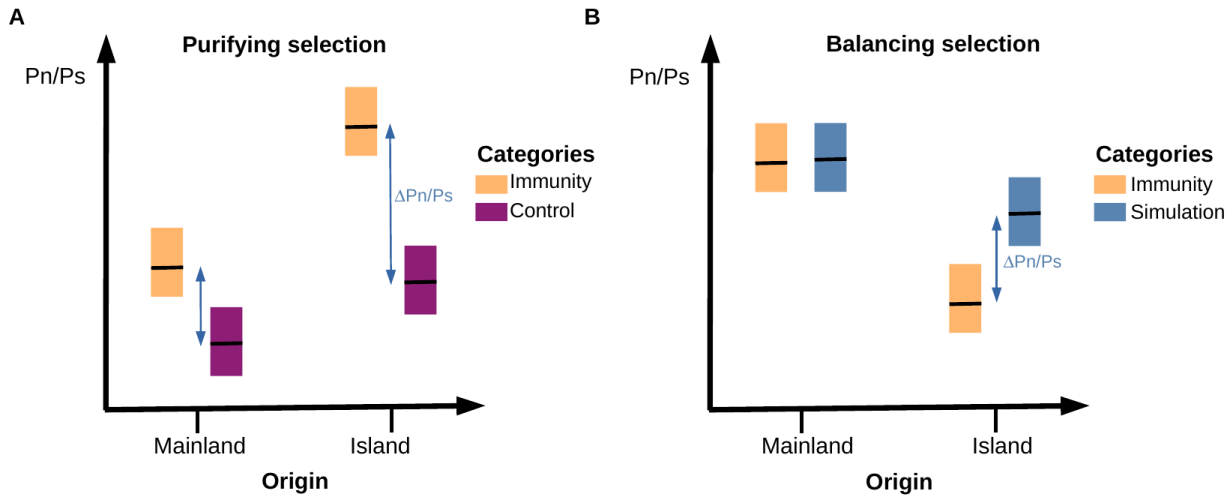

Figure 2: Conceptual diagram showing the expected results under the hypothesis of a relaxation in the selection pressure of the immune genes in island species due to a change in the parasitic community. A) Genes evolving under purifying selection where control genes are randomly selected protein-coding genes. B) Genes evolving under balancing selection where controls are obtained from SLiM simulations of genes evolving under the same balancing selection but different population size. Under the hypothesis of a relaxed selection as a consequence of the reduced diversity of pathogens on island ecosystems, the difference in Pn/Ps between categories (ΔPn/Ps) is expected to be different between species' origin, leading to a statistical interaction between gene categories and origin.

Methods

Dataset

Alignments of Coding DNA Sequences (CDS) of individuals from 24 species were obtained from Leroy et al. (2021b). In addition, data for ten other species (six and four from islands and mainland, respectively) were newly generated for this study by targeted-capture sequencing. Blood samples and subsequent DNA extractions were performed by different research teams. The complete dataset consisted of 34 bird species (20 and 14 insular and mainland species respectively; Table 1; Figure 1). We filtered alignments in order to retain only files containing a minimum of five diploid individuals per site (Table 1).

Sequence enrichment was performed using MYBaits Custom Target Capture Kit targeting 21 immune genes: 10 Toll-Like receptors (TLR), 9 Beta Defensins (BD), 2 Major

195 Histocompatibility Complex (MHC) and 97 control genes (see below). We followed the
196 manufacturer's protocol (Rohland and Reich, 2012). Illumina high-throughput sequencing
197 using a paired-end 150 bp strategy was performed by Novogene (Cambridge, UK).

198

199 Table 1: List of species and sampling localities, along with the type of data obtained and the
200 number of individuals (N).

Species	Origin	Island/Country	N	Reference genome	Reference for population genomics data	Type of data
Cyanistes teneriffae palmae	Island	La Palma	15	*Cyanistes caeruleus* (This study)	(Mueller et al., 2016)	Capture
Cyanistes teneriffae teneriffae	Island	Tenerife	14			
Cyanistes caeruleus	Mainland	France	15			
Parus major	Mainland	Europe	10	*Parus major* (Laine et al., 2016)	(Corcoran et al., 2017)	Whole genome
Phylloscopus trochilus	Mainland	Europe	9	*Phylloscopus trochilus* (Lundberg et al., 2017)	(Lundberg et al., 2017)	Whole genome
Zosterops virens	Mainland	South Africa	7	*Zosterops borbonicus* (Leroy et al., 2021a)	(Leroy et al., 2021b)	Whole genome
Zosterops olivaceus	Island	Réunion	15			
Zosterops mauritianus	Island	Mauritius	9			
Zosterops borbonicus	Island	Réunion	25			
Ficedula semitorquata	Mainland	Europe	20	*Ficedula albicollis* (Ellegren et al., 2012)	(Ellegren et al., 2012)	Whole genome
Ficedula albicollis	Mainland	Europe	20			
Ficedula speculigera	Mainland	Nord Africa	20			
Ficedula hypoleuca	Mainland	Europe	20			
Turdus olivaceofuscus	Island	São Tomé	15	*Turdus pelios* (This study)	This study	Capture
Turdus pelios	Mainland	Gabon	15			
Cyanomitra olivacea	Island	Príncipe	15	*Cyanomitra olivacea* (This study)	This study	Capture
Cyanomitra olivacea	Mainland	Gabon	15			
Ploceus grandis	Island	São Tomé	13	*Ploceus cucullatus* (This study)	This study	Capture
Ploceus princeps	Island	Príncipe	13			
Ploceus nigerrimus	Mainland	Cameroon Gabon	14			
Poephila acuticauda acuticauda	Mainland	Australia	10	*Taeniopygia guttata* (Warren et al., 2010)	(Singhal et al., 2015)	Whole genome
Taeniopygia guttata castanotis	Mainland	Australia	19			
Fringilla teydea	Island	Tenerife	10	*Fringilla coelebs* (Recuerda et al., 2021)	(Leroy et al., 2021b)	Whole genome
Fringilla canariensis palmae	Island	La Palma	15			
Fringilla coelebs	Mainland	Spain	9			
Certhidea olivacea	Island	Santiago (Galápagos)	5	*Geospiza fortis* (Zhang et al., 2012)	(Lamichhaney et al., 2015)	Whole genome
Certhidea fusca	Island	San Cristobal (Galápagos)	10			
Certhidea fusca	Island	Española (Galápagos)	10			
Geospiza difficilis	Island	Pinta(Galápagos)	10			
Platyspiza crassirostris	Island	Santa Cruz (Galápagos)	5			
Pinaroloxias inornata	Island	Coco (Galápagos)	8			
Camarhynchus pallidus	Island	Santa Cruz (Galápagos)	5			
Geospiza difficilis	Island	Wolf (Galápagos)	8			
Geospiza conirostris	Island	Española (Galápagos)	10			

201

Newly generated draft genome sequence

We generated whole genome sequences at moderate coverage (~40X) for *Turdus pelios*, *Ploceus cucullatus* and *Cyanomitra olivacea* (from Gabon). Library preparation from blood DNA samples and Illumina high-throughput sequencing using a paired-end 150 bp strategy were performed at Novogene (Cambridge, UK). Raw reads were cleaned using FastP (vers. 0.20.0; Chen et al., 2018). Genomes assemblies were performed using SOAPdenovo (vers. 2.04) and Gapcloser (v1.10) (Luo et al., 2012) with parameters "-d 1 -D 2" and a kmers size of 33. Protein annotation was performed by homology detection using genBlastG (She et al., 2011; http://genome.sfu.ca/genblast/download.html) and the transcriptome of the collared flycatcher (*Ficedula albicollis*; assembly FicAlb1.5; Ellegren et al., 2012) as reference.

Capture data processing

Reads from targeted-capture sequencing were cleaned with FastP (vers. 0.20.0; Chen et al., 2018). Reads of each individual were mapped respectively to the nearest available reference genomes using bwa mem (vers. 0.7.17; Li, 2013; Table 1), with default parameters. Samtools (vers. 1.3.1; Li et al., 2009) and Picard (vers. 1.4.2; Picard Toolkit 2019) were used to convert the mapping files, order and index reads according to their position on the chromosomes (or scaffolds) of the reference genomes or on the draft genomes generated in this study for *Ploceus*, *Cyanomitra* and *Turdus*. Duplicate reads were marked using MarkDuplicates (vers. 1.140; Picard Toolkit 2019). SNP calling was performed with Freebayes (vers. 1.3.1; Garrison and Marth, 2012). Freebayes output file (VCF file) was converted to a fasta file by filtering out sites with a minimum quality of 40 and a sequencing depth between 10 and 1000X (sites outside these thresholds were treated as missing data, i.e., 'N'). CDS were then extracted from the alignments using the coordinates of the annotations (gff files). CDS were aligned using MACSE (vers. 2.03; Ranwez et al., 2011) to prevent frameshift mutation errors and GNU-parallel (Tange, 2018) was used to parallelise the computation.

Selection and identification of immune and control genes

We defined several groups of immune genes to compare with the control genes. The control group consisted of 97 protein-coding genes randomly selected in the genome of *Zosterops borbonicus* (Leroy et al., 2021a). These control genes allowed the estimation of the average selection pressure that a gene, not involved in the immune response, undergoes in the genome.

233 These genes are single copy (absence of paralogue) and have a variable GC content
234 representative of the whole transcriptome.

235 For the immune genes, we selected three sets of genes from i) a limited set of genes (Core
236 Group) where functions are unambiguously related to immunity, and ii) two larger sets of genes
237 (Database-group & Sma3s-group), obtained through an automatic annotation pipeline.

238 The Core Group included MHC class I and class II genes, 10 Toll-Like Receptors (TLRs;
239 Velová et al., 2018) and 9 Beta Defensins (BD; Chapman et al., 2016). The Database group
240 included genes identified by Immunome Knowledge Base (Ortutay and Vihinen, 2009,
241 http://structure.bmc.lu.se/idbase/IKB/; last access 04/02/2020) and InnateDB (Breuer et al.,
242 2013, http://www.innatedb.com ; last access 04/02/2020). We also added a set of genes for
243 which the genetic ontology indicated a role in immune functions. To do so, we used the chicken
244 (*Gallus gallus*) annotation (assembly GRCg6a downloaded from Ensembl database in March
245 2020; https://www.ensembl.org/). We identified genes with the terms "immun*" or
246 "pathogen*" in their Gene Ontology identifiers description (directory obtained from
247 http://geneontology.org/). This set included 2605 genes considered to be involved in immunity,
248 although some may be only indirectly involved in immunity or have a small impact on immune
249 functions. Finally, the third set of genes (Sma3s-group) has been built up through the Sma3s-
250 group program (vers. 2; Munoz-Mérida et al., 2014). This program annotated sequences in
251 order to be associated with biological functions through gene ontology identifiers. The
252 annotation of the genome of *F. albicollis* allowed us to identify 3136 genes associated with the
253 genetic ontology "immune system processes". Like for the Database group, this set may include
254 genes with various functions in the immune response. It should be noted that Sma3s-group and
255 Database-group are not mutually exclusive, and some genes are present in both groups. An
256 analysis was performed to identify and exclude genes under balancing selection from Database-
257 group and Sma3s-group sets using BetaScan (vers. 2; Siewert and Voight, 2020), due to the
258 potentially antagonistic responses of these genes. Very few genes (only 2 and 3 genes from
259 Database-group and Sma3s-group sets) were identified and removed from the analysis (see
260 Detection of genes under balancing selection in Supplementary Methods).

261 *Test for contamination and population structure*

262 We use the program CroCo (vers. 1.1; Simion et al., 2018) to identify candidates for cross-
263 species contamination (see supplementary materials for details). Overall, we did not detect a

264 clear case of cross-species contamination in our dataset (Figure S1). Contigs identified as
265 potential contamination always involve a pair of species belonging to the same genus. In this
266 case, contamination could be difficult to identify due to the low genetic divergence between
267 species.

268 For the newly sequences species, we also performed PCA analyses on using allele frequencies
269 of control genes. We use the function dudi.pca of adegenet R packages (Jombart and Ahmed,
270 2011). This analysis aims to check for population structure and to detect potentially
271 problematic individuals (i.e., contaminated individuals). This analysis led to the exclusion of 4
272 individuals (*Ploceus princeps* P6-174; *P. grandis* ST10_094; *P. nigerrimus* G3_016; *C.*
273 *teneriffae* TF57) for which we suspected contamination. Otherwise, no extra population
274 structure was detected (Figure S2-S4).

275 *Hidden paralogy*

276 We compute the statistic Fis = 1-H0/He where H0 is the average number of heterozygous
277 individual observed (H0 = #heterozygous / n ; where n is the sample size) and He is the
278 expected number of heterozygous individuals at Hardy-Weinberg (HW) equilibrium (He =
279 (n/(n-1) 2 * p * (1-p))*n where n is the sample size and p the allele frequency of a randomly
280 chosen allele). Fis varies between -1 and 1 with positive value representing excess of
281 homozygous individuals and negative value representing excess of heterozygous individuals
282 compared to the HW proportions. Gene with high value of nucleotide diversity (Pi) and
283 negative value of Fis could represent potential cases where hidden paralogous sequences have
284 not been separated and where all the individuals present heterozygous sites in the positions
285 where a substitution occurred between the paralogous copies. Five TLR21 genes appear
286 problematic (Pi > 0.01 and Fis < -0.5; Figure S5) and were excluded from further analyses.

287 The MHC genes are more difficult to analyse. Indeed, heterozygosity could be comparable to
288 divergence under balancing selection. This makes the identification of orthologs very difficult.
289 We identify a variable number of genes among species (from 1 to 10 genes for MHC class I
290 and MHC class II). We checked the sequence similarity for the 10 copies of the MHC class II
291 in *F. albicollis* and the 7 copies of the MHC classI genes in *C. caeruleus* using cd-hit (Fu et
292 al., 2012). For MHC class II, sequence divergences ~~are~~ always higher than 15% indicating that
293 reads will likely be correctly assigned to their corresponding gene copy. For MHC class I,
294 sequence identities could be as high as 95%. In this case, we rely on the fact that the reads from

very similar paralogous copies will not be confidently assigned to a gene copy sequence by the mapping software. This will lead to a low mapping score quality and are likely to be discarded during the genotype calling procedure. For example, 3 out of 7 genes of the *Cyanistes* MHC class I genes could not have been correctly genotyped and are missing from our final dataset.

Data Analysis

SLiM simulations

We use SLiM (vers. 3.3.2; Haller and Messer, 2017) to estimate the impact of demographic changes on polymorphism patterns under various selection regimes. The following parameters were used in all simulations. Sequences of 30kb with a mutation of $4.6e^{-9}$ substitutions/site/generation were simulated (Smeds et al., 2016). Recombination was set to be equal to mutation rate. Introns/exons pattern was reproduced by simulating fragments of 3kb separated by one bp with a very high recombination rate of 0.1 rec./site/generation. Five types of mutations were possible: i) neutral synonymous mutations, ii) non-synonymous mutations with a Distribution of Fitness Effect (DFE) following a gamma law of mean = -0.025 and shape = 0.3, which corresponds to the DFE estimated in Passerines by Rousselle et al. (2020), iii) codominant non-synonymous mutations positively selected with s = 0.1, iv) non-synonymous mutations under balancing selection with an effect on fitness initially set at 0.01 but re-estimated by the program at each generation according to the mutation frequency in the population, thus including a frequency-dependent effect and v) non-synonymous mutations under overdominance using with a dominance coefficient of 1.2.

We simulate a coding sequence organization where positions one and two of the codons were considered as non-degenerated sites, with the non-synonymous types of mutations previously described are possible in various proportions. The third position was considered as completely neutral where only synonymous mutations could appear.

In the absence of control genes evolving under balancing selection, we use SLiM to generate a set of control genes for this category. We simulate two populations of 270,000 and 110,000 individuals, representing mainland and island effective population size respectively.

We also explore the effect of positive and balancing selection on the pattern of Ps and Pn/Ps in a population of size 50,000, 110,000, 270,000 and 500,000. In order to speed up the computational time, we ~~reduce~~ the population size by a factor 100 and ~~rescale~~ mutation rate, recombination rate and selection coefficient accordingly.

326 All the details of the simulation parameters, calculations of non-synonymous polymorphism
327 rate (Pn) and synonymous polymorphism rate (Ps) of simulated sequences, as well as SLiM
328 command lines are provided in Supplementary Methods and Supplementary Materials.

329 *Polymorphism analyses*

330 Synonymous (Ps) and non-synonymous (Pn) nucleotide diversity were estimated from
331 seq_stat_coding written from the Bio++ library (Available as Supplementary data; Guéguen et
332 al., 2013). The mean Pn/Ps was computed as the sum of Pn over the sum of Ps (Wolf et al.,
333 2009). Ps of concatenated sequences of control genes were estimated for each species of our
334 dataset. For the whole-genome sequence species, we compared the Pn/Ps and Ps estimated
335 obtained using the 97 control genes with the values from Leroy et al., (2021b; ~5000 genes
336 used in their study). Pn/Ps and Ps correlations showed a R of 0.6 and 0.95 respectively (Figure
337 S6). Thus, the 97 control genes used in our study were representative of a larger set. This
338 allowed us to identify *Phylloscopus trochilus* as an outlier. Unlike for all other species (e.g.
339 *Fringilla coelebs*, Figure S7), synonymous polymorphism level was correlated to the amount
340 of missing data in *P. trochilus* alignments (Figure S7). As such, we excluded *P. trochilus* from
341 further analysis.

342 The mean Pn/Ps, calculated from the concatenated sequences of genes from the same gene
343 class (control genes; BD; TLR; MHC I; MHC II; Database-group; Sma3s-group), was
344 estimated for each bird species. Alternative transcripts were identified based on the genomic
345 position in the GFF file. If several transcripts were available, one transcript was randomly
346 selected. Pn/Ps estimates based on less than four polymorphic sites were excluded from the
347 analysis, as were those with no polymorphic non-synonymous sites.

348 *Statistical analyses*

349 To estimate the impact of demographic history on genome-wide polymorphism of island
350 species and the potentially reduced constraints on their immune genes, we computed the ratio
351 of non-synonymous nucleotide diversity over synonymous nucleotide diversity (Pn/Ps). A
352 linear mixed model was performed, using the Pn/Ps ratio as dependent variable and, as
353 explanatory variables, the mainland or insular origin of species as well as the category of genes
354 (packages lme4 and lmerTest (Bates et al., 2012; Kuznetsova et al., 2017)). In order to take the
355 phylogenetic effect into account, the taxonomic rank "family" was included as a random effect
356 in the model. We also used a generalized linear mixed model (using the function glmer of the

357 package lme4) with the family “Gamma(link="log")” which leads to the same results (Figure
358 S15 to S24). Five linear mixed models were defined i) null model, ii) model with only the
359 origin parameter, iii) model with only the gene category parameter, iv) model using both origin
360 and gene category parameters, and finally v) model including those two parameters and the
361 interaction effect. In some cases, the phylogenetic effect was difficult to estimate because the
362 number of species per family was reduced to one. In that case, we chose to reduce the number
363 of families by grouping Turdidae with Muscicapidae, Nectariniidae, and Estrildidae with
364 Ploceidae and Fringillidae within Thraupidae. The results obtained with these family groupings
365 were similar to the original model (Table S1), except when stated. The categories Database-
366 group and Sma3s-group were tested separately from the Core group because they contained
367 hundreds of genes annotated using the automatic pipeline that were only available for species
368 with genome wide data. Database-group and Sma3s-group were not analysed simultaneously
369 because they contained a partially overlapping set of genes. Finally, genes evolving under
370 purifying selection and genes evolving under balancing selection were also analysed
371 separately. Model selection was based on two methods. First, we use the difference in corrected
372 Akaike Information Criterion (ΔAICc) calculated using the qpcR package (Spiess and Spiess,
373 2018). Second, a model simplification using an ANOVA between models was also performed.

374 We also tested an alternative model using the difference between Pn/Ps of immune genes and
375 control genes (*Δ*Pn/Ps) as dependent variable, and species origin as explanatory variable. Under
376 the hypothesis of a relaxation in selection pressure on islands due to a change in the parasite
377 community, we expect the *Δ*Pn/Ps to be higher on island species compared to the mainland
378 ones and, therefore, the species origin (i.e., mainland or island) to be significant. In this model,
379 we used the Phylogenetic Generalized Least Squares model (PGLS; implemented in the “nlme”
380 packages; Pinheiro et al., 2017). This model assumes that the covariance between species
381 follows a Brownian motion evolution process along the phylogeny (implemented using the
382 “corBrownian” function from the ‘“ape”’ package; Paradis and Schliep, 2019). The species
383 phylogeny was estimated using mitochondrial genes and a maximum likelihood inference
384 implemented in IQTREE (model GTR+Gamma and ultrafast bootstrap; Nguyen et al., 2014;
385 median of 11,134 bp analysed per species). The phylogeny with the bootstrap support is
386 provided as supplementary material.

All the statistical analyses were performed using R (R Core Team, 2018), and dplyr package (Wickham, 2016). Graphical representations were done using ggplot2, ggrepel, ggpubr and ggpmisc (Aphalo, 2020; Kassambara, 2018; Slowikowski et al., 2018; Wickham, 2016).

Results

For the 150 individuals (10 species with 15 individuals each) for which we generated new data by targeted capture sequencing, an average of 3.3 million paired-ends reads per individual was generated (Table S1). After mapping, genotyping and cleaning, we analysed 86 control and 16 immune genes on average per species, out of the 141 targeted genes (120 control and 21 immune related genes; Table S4). For the species with whole-genome sequences, we analysed 106 control and 20 immune genes on average per species, out of the 141 targeted genes, and 875 and 688 genes on average in the Database-group and Sma3s-group respectively (Table S4).

For the species for which full genome sequences were available, the Ps and Pn/Ps estimated using the control genes reflect the Ps and Pn/Ps of the whole transcriptome (Figure S6).

Population genetics of BD and TLR Immune genes

In order to characterize the selection regimes shaping the BD and TLR polymorphisms, we first analyze the variation of Pn/Ps ratios among gene categories using a linear mixed model.

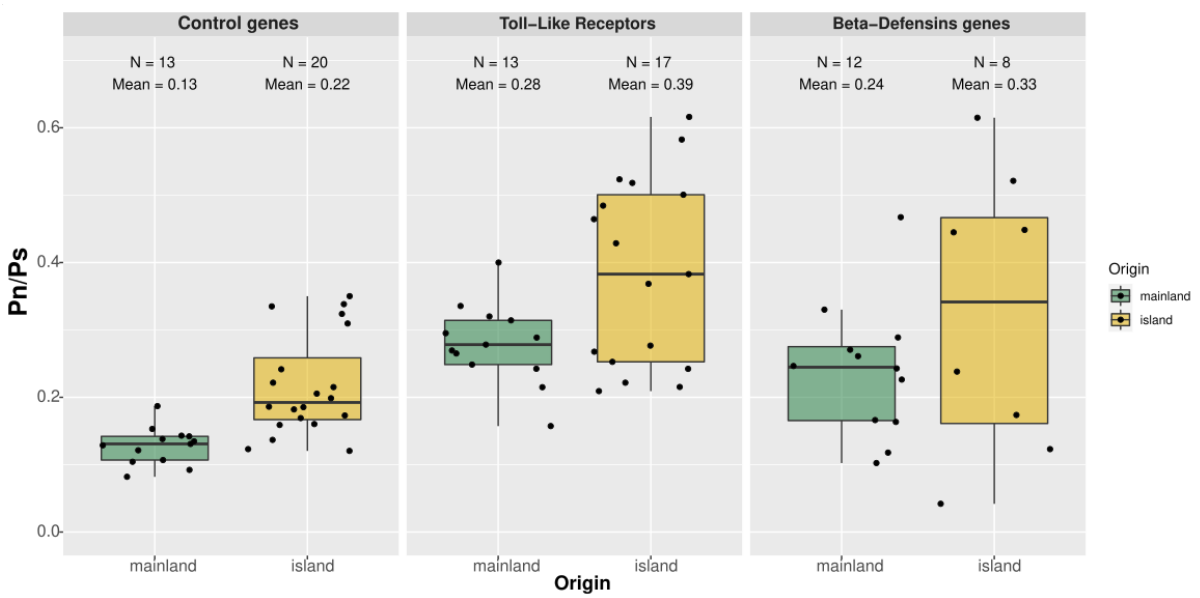

Figure 3: Pn/Ps according to species origin (mainland in green and insular in orange) for different gene categories under purifying selection. The number of species (N), and the mean Pn/Ps are shown for each modality.

Model selection based on AICc as well as model selection approach based on simplification with ANOVA identified the model including the origin (i.e., mainland or island) and gene category without interaction (Table 2). In this model, island origin of species is associated with a greater Pn/Ps (0.14 vs. 0.10; Table 3; $p < 0.01$). Gene categories corresponding to TLRs and BDs showed a significantly higher Pn/Ps than control genes (Table 3; $p < 0.001$). Our statistical analysis confirms that island birds have a higher Pn/Ps ratio than mainland relatives, in agreement with the nearly-neutral theory of evolution. It also reveals that immune genes have a higher Pn/Ps than randomly selected control genes suggesting that BD and TLR evolve under a different selection regime than non-immune related genes.

Next, we investigate the cause of the higher Pn/Ps of immune genes by testing three hypotheses. First, we exclude a bias due to a lower number of genes in immune genes, and therefore higher variance in the estimation of Pn/Ps, in immune genes. Immune genes still have significantly higher Pn/Ps compared to a random subsample of control genes of comparable size (Figure S8 & S9). Second, the Pn/Ps of immune genes could be inflated by positive selection. It is well known that immune genes are subject to frequent adaptation due to harm race evolution with pathogens (Enard et al., 2016; Shultz and Sackton, 2019; Velová et al., 2018). We evaluate the effect of positively selected genes on the Pn/Ps using SLiM simulations with both positively and negatively selected mutations. The presence of recurrent positive selection could increase the Pn/Ps leading to a higher Pn/Ps in immune genes if this category is more prone to adaptive evolution (Figure 4A). However, positive selection always leads to a drastic decrease in Ps due to genetic sweep effect at linked sites (Figure 4B). BDs and TLRs have a slightly higher or similar Ps than control genes (Figure S9, mean Ps = 0.007, 0.004 and 0.003 for BDs, TLRs and control genes respectively, effect of gene category $p < 0.1$) and, as a consequence, even if positive selection is likely to have impacted the evolution of immune genes, it is not the cause of the higher Pn/Ps observed here. Third, balancing selection could be present, at least temporarily, in the evolution of BDs and TLRs genes (Kloch et al., 2018; Levy et al., 2020). Simulation analyses confirm that balancing selection causes an increase of Ps and Pn/Ps (Figure 4C & 4D). However, a change in effective population size has an opposite effect on the Pn/Ps according to the type of selection. In the presence of slightly deleterious mutations, Pn/Ps decreases with *Ne* whereas it increases in the presence of balancing selection. Island birds have

438 higher Pn/Ps ratios than mainland birds for BDs and TLRs. Therefore, we can rule out
439 balancing selection as the main factor explaining the high Pn/Ps of immune genes because, in
440 this case, Pn/Ps of island birds should be lower. The last possible explanation we can think of
441 is a relaxed selection of immune genes. It is likely that immune genes are overall less
442 constrained than the control genes. It has been shown that evolutionary constraints are more
443 related to gene expression than to function (Drummond et al., 2005; Drummond and Wilke,
444 2008) and therefore, functionally important genes could still have a high Pn/Ps.

445 Overall, our analyses do not support a strong impact of ongoing adaptive mutation or balancing
446 selection on BDs and TLRs. However, these immune genes do not evolve as the random genes
447 not involved in immune functions and present a significantly higher Pn/Ps of 0.20 ($p < 0.001$;
448 Table 3).

449 *No evidence of a reduced impact of the parasite communities on the polymorphism pattern*
450 *immunes genes in island birds*

451 For BDs and TLRs, the best model selected includes the origin (i.e., mainland or island) and
452 gene category without interaction (see above and Table 2). This model has no interaction
453 between origin and gene categories invalidating the hypothesis of a reduced parasite
454 communities on island (Figure 2).

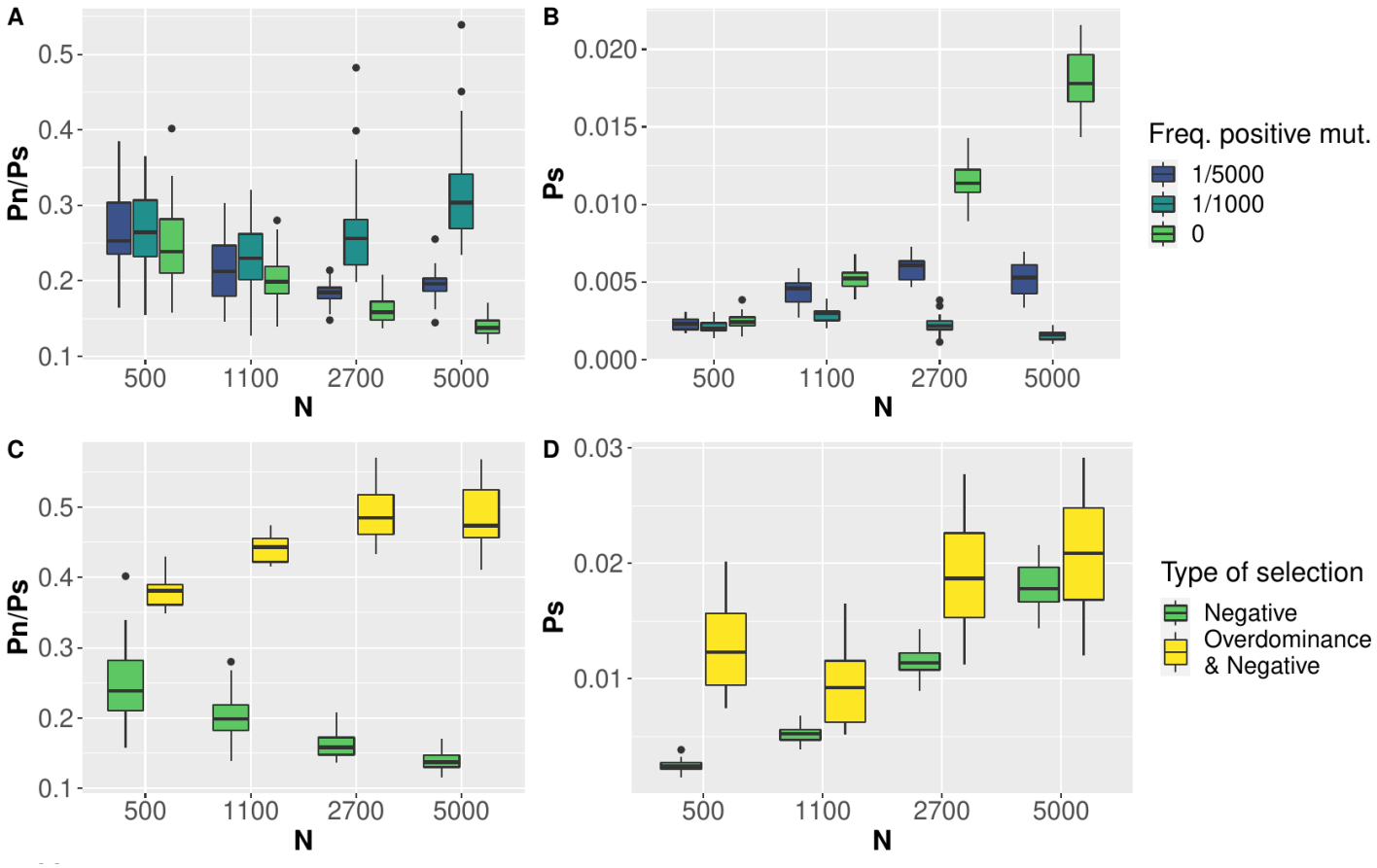

Figure 4: Neutral polymorphism (Ps) and ratio of selected over neutral polymorphism (Pn/Ps) estimated from SLiM simulations. A) Pn/Ps as a function of population size, N and B) Ps as a function of N. In both A and B, colour indicates the frequency of positively selected mutation compare to deleterious mutation. C) Pn/Ps as a function of N and D) Ps as a function of N. In both C and D, yellow indicates simulations with overdominance mutation (h = 1.2) and negatively selected mutations and green indicates simulations with only negatively selected mutations.

Table 2: Statistical model explaining Pn/Ps variation of Toll-Like Receptors, Beta-Defensins genes, and control genes. The p-values of ANOVA test between simpler models are not reported if a more complex model explains a larger proportion of the variance.

Model		Model selection by AIC			ANOVA test			
n°	Details	AICc	ΔAICc	Likelihood	n° 1	2	3	4
1	Pn/Ps~ 1+ category +origin+	-5.39	8.83	0.01		0.63		

	category *origin					
2	Pn/Ps~ 1+ category +origin	-14.22	0	1	0.002	3.71E-05
3	Pn/Ps~1+ category	-11.8	2.42	0.3		
4	Pn/Ps~1+ origin	-6.83	7.39	0.02		
5	Pn/Ps~1	-6.44	7.78	0.02		

468

469 Table 3: Summary of the best statistical model selected using AICc explaining variation in
470 Pn/Ps in control genes, Toll-Like receptors and Beta-Defensins genes under purifying selection
471 with origin, gene category parameters. * indicates significances : * < 0.05; ** < 0.01; *** <
472 0.001.

Model	*Parameters*			*Estimate*	*P.value*	
		Origin	*Category*			
Origin and Gene category (n°2)	*Intercept*	*mainland*	*Control genes*	*0.10*	*2.65E-02*	*
		island		*0.14*	*4.56E-03*	**
			Toll-Like Receptors	*0.20*	*7.43E-05*	***
			Beta-Defensins genes	*0.20*	*3.16E-04*	***

473

474 For larger sets of genes, identified using an automatic pipeline and gene annotation, model
475 selection based on AICc and simplification with ANOVA (Table S5, S8) identified models
476 that included origine parameters which associated a higher Pn/Ps of at least 0.07 for island
477 species (p < 0.001; Table S6, S7, S9, S10, Figure 5). Selection model by simplification with
478 ANOVA identified models with interaction effect between origin and gene category associated
479 with a reduced Pn/Ps for immune genes of island species that invalidate our hypothesis (Table
480 S7, S10).

481

482 The alternative statistical approach using the difference between Pn/Ps of immune genes and
483 control genes (ΔPn/Ps) as dependent variable, and species origin as explanatory variable under
484 a PGLS framework lead to similar results. Island was never associated to a statistically higher
485 ΔPn/Ps (table S2) providing no support for an increased relaxed selection of immune genes in
486 island species.

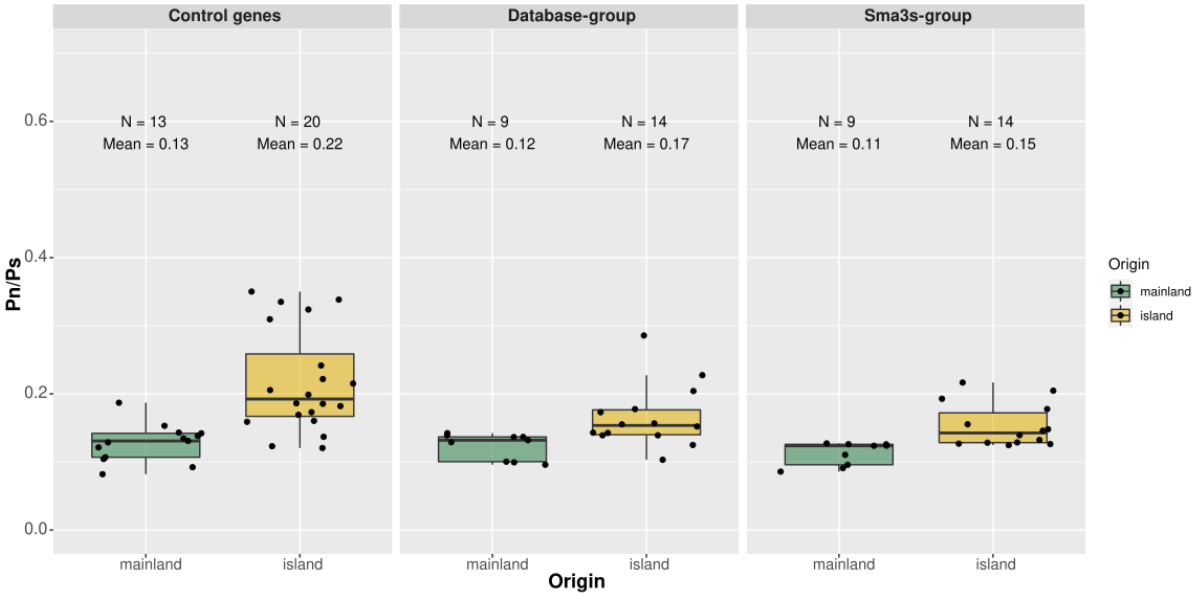

Figure 5: Boxplot of Pn/Ps according to species origin (mainland in green and insular in orange) for different gene categories under purifying selection. The number of individuals (N), and the mean Pn/Ps are shown for each modality.

Genes under balancing selection

First, we estimated the effect of population size variation on the Pn/Ps of the genes evolving under balancing selection by simulating sequences under frequency dependent or overdominance selection using SLiM (see Methods and Supplementary Methods). The simulation under frequency dependence selection revealed an average Pn/Ps equal to 0.8 for island species and 1.2 for mainland species (Figure 6). Under overdominance, simulated sequences from island and mainland populations respectively have an average Pn/Ps equal to 0.54 and 1.03 (Figure 6).

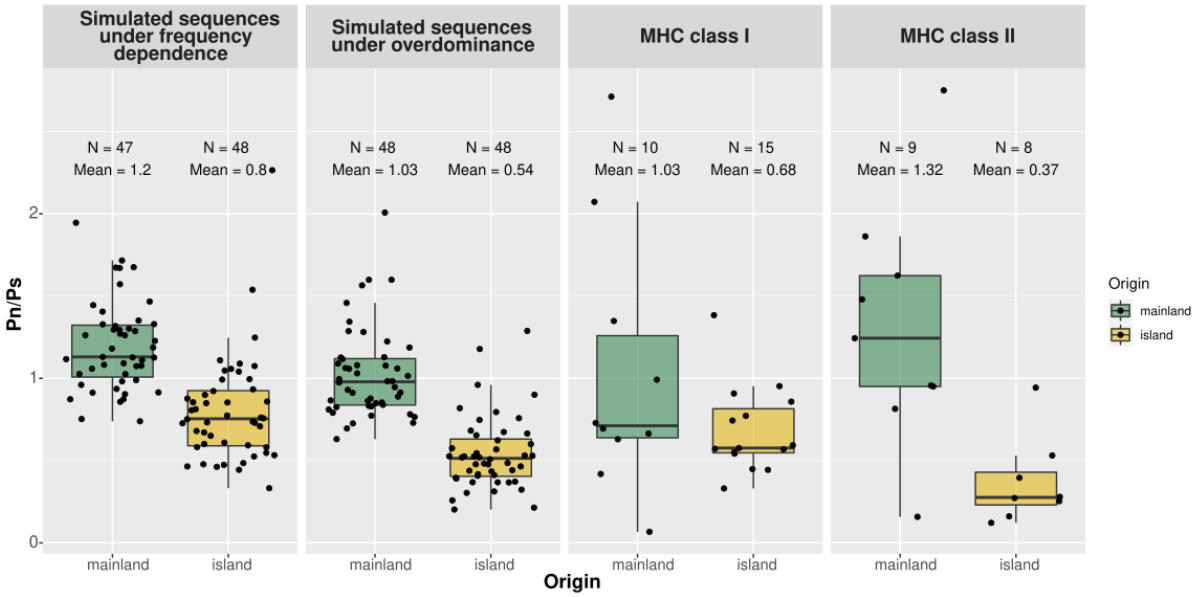

Figure 6: Boxplot of Pn/Ps according to species origin (mainland in green and insular in orange) for different gene categories under balancing selection. The number of species (N), and the mean Pn/Ps are shown for each modality. The control groups correspond to the results obtained from simulated sequence via SLiM (see Methods and Supplementary Methods Simulation of control genes under balancing selection).

Using simulations under frequency ~~dependence~~ selection as well as simulations under the overdominance, model selection by AIC identifies the model with origin as the best, contrary to the method by simplification with ANOVA which identified the full model therefore including significant interaction between origin and genes category (Table 4). This interaction effect is significant for the MHC II ($p < 0.05$, Table S12) but not for MHC I. As expected, island species have a significantly lower Pn/Ps in MHC genes compared to mainland species ($p < 0.01$; except for the full model based on control genes evolving under overdominance Table S12).

Table 4: Statistical model explaining Pn/Ps variation of genes under balancing selection (i.e MHC class I and II), and simulated sequences under i) frequency dependence or ii) overdominance. The p-values of ANOVA test between simpler models are not reported if a more complex model explains a larger proportion of the variance.

Model			Model selection by AIC			ANOVA test			
Type of balancing selection	n°	Details	AICc	ΔAICc	Likelihood	n°1	2	3	4

Frequency dependence	1	Pn/Ps~1+ category +origin+ category *origin	157.17	5.62	0.06	0.019
	2	Pn/Ps~1+ category +origin	157.85	6.31	0.04	
	3	Pn/Ps~1+ category	187.58	36.04	0.00	
	4	Pn/Ps~1+ origin	151.54	0.00	1.00	
	5	Pn/Ps~1	180.52	28.97	0.00	
Overdominance	1	Pn/Ps~1+ category +origin+ category *origin	140,56	8,50	0,01	0.024
	2	Pn/Ps~1+ category +origin	140,56	8,50	0,01	
	3	Pn/Ps~1+ category	185,91	53,85	0,00	
	4	Pn/Ps~1+ origin	132,05	0,00	1,00	
	5	Pn/Ps~1	177,54	45,49	0,00	

Discussion

On oceanic islands, the depauperate parasite community is expected to lead to a relaxation of selection on the immune system. In this study, we found support for such an effect, but only on MHC class II genes and using simulated sequences under balancing selection as control. No effect was detected for MHC class I genes nor for innate immune genes (TLRs and BDs), evolving under purifying selection. On these gene sets, increased drift effects on island populations limit the efficacy of selection in accordance with the nearly-neutral theory (Ohta, 1992). The ability to distinguish between the selective and nearly-neutral processes (relaxed selection due to environmental change vs. drift) could only be achieved by our approach of using random genes (i.e., “control genes") to estimate the genome-wide effect of potential variation in effective population size between populations.

Effects of effective population size variation

Our results support the nearly-neutral theory of evolution for those genes under purifying selection, whereby strong genetic drift acting on small island populations reduces the efficacy of natural selection, leading to an increase in non-synonymous nucleotide diversity compared to the mostly neutral, synonymous nucleotide diversity (i.e., Pn/Ps; Ohta, 1992). This is materialized by a genome-wide increase in frequency of weakly deleterious mutations (Kutschera et al., 2020; Leroy et al., 2021b; Loire et al., 2013; Robinson et al., 2016; Rogers and Slatkin, 2017).

For genes evolving under balancing selection, we performed simulations under the hypotheses of overdominance (heterozygote advantage) or frequency dependence (rare-allele advantage). Our results showed reduced Pn/Ps for smaller population sizes (Figure 6, S10, S11). This simulation confirmed our expectations (Figure 2) that a reduction in the efficacy of selection results in a decrease in the frequency of non-synonymous polymorphism, as, under normal circumstances, selection maintains those mutations at intermediate frequencies. It also matches what we obtained in the empirical results, where both MHC classes I and II had a reduced Pn/Ps in island birds. This result supports that the fitness effect of having non-synonymous polymorphisms segregating at high frequencies is not strong enough to counteract entirely the effect of genetic drift on islands, therefore extending the nearly-neutral theory to the overdominance type of selection.

Effects of selection on immune genes

For immune genes, we try to characterize the nature of the selection acting on BDs and TLRs genes. Comparing those genes with control genes and using simulations, we were able to rule out that directional positive selection and balancing selection had a major impact shaping the polymorphism of these immune genes. In contrast, the pattern of Pn/Ps between island and mainland populations is in line with the effect of purifying selection in the presence of slightly deleterious ~~mutation~~. However, no effect was detected on insular species, beyond what could be attributed to genetic drift. This is in line with the result of Gonzalez-Quevedo et al. (2015b) and Grueber et al. (2013) who found that TLR genetic diversity was mostly influenced by genetic drift. At first sight, this result seems not in line with the fact that island parasite communities are less diverse (Beadell et al., 2006; Loiseau et al., 2017; Maria et al., 2009;

Pérez-Rodríguez et al., 2013; but see Illera et al., 2015). However, a reduced ~~pathogens number~~ has also been found to be associated with a higher prevalence in birds and reptiles from the Macaronesian archipelago (Illera and Perera, 2020). Therefore, these two patterns, i.e. a less diverse pathogen's community on islands with a higher prevalence, could still imply a strong selection pressure on immune genes.

In contrast, for MHC genes that unambiguously evolve under balancing selection, MHC class II genes presented a reduction in non-synonymous polymorphism larger than the effects of drift alone, when simulated sequences are used as control. This was the only case where a role for relaxed selection pressures in the molecular evolution of immune genes could be invoked.

Our results are in accordance with the hypothesis of Lee (2006), which proposes that innate and acquired immunity may exhibit distinct responses to changes in pressures due to different costs and benefits. However, our result contrast~~s~~ with the study of Santonastaso et al. (2017) that identified no change in selection pressures on MHC II genes in a lizard species, concluding that their evolution was mostly governed by drift. Similarly, Agudo et al. (2011) also found a prominent role for genetic drift over selection in the evolution of MHC II genes in the Egyption vulture (*Neophron percnopterus*).

Our results rely on simulations that may be affected by the choice of the parameter values. First, we performed simulations using a fixed effective population size (*Ne*) estimated from the polymorphism data. Using others values of *Ne* had a weak impact on the relative difference between island and mainland species for the overdominance type of selection (Figure S10, S11). Secondly, we simulated two types of selection, namely overdominance (Doherty and Zinkernagel, 1975) and frequency dependence (Slade and McCallum, 1992), but it has been argued that the maintenance of MHC polymorphism could be the result of fluctuating selection (Hill, 1991). Additionally, recombination ~~&~~ gene conversion has also been put forward as a mechanism responsible for generating diversity (Spurgin et al., 2011). Therefore, our results for the MHC II, which is based on the relative difference between Pn/Ps of island and mainland species comparing empirical and simulated data, should be taken cautiously as their significance can be dependent on the specific parameters that we used, although we did our best to select a realistic range of parameters.

The observed difference between MHC class I and II could be explained by their different pathogen targets: MHC class I genes are primarily involved in the recognition of intracellular

592 pathogens (Kappes and Strominger, 1988), while MHC class II genes are directly involved in
593 the recognition of extracellular pathogens (Bjorkman and Parham, 1990). These differences
594 could lead to variable selection pressures depending on the extracellular versus intracellular
595 parasite communities present on islands. In addition, the relaxed selection pressures on MHC
596 II genes from adaptive immunity is in line with a reduction in acquired immunity parameters
597 observed by Lobato et al. (2017) that used partly the same sets of species.

598 As a perspective of our work, we should mention that there is an extensive variation in the
599 number of MHC gene copies across the avian phylogeny (Minias et al., 2019; O'Connor et al.,
600 2020). Particularly, it was recently discovered that Passerines have a very dynamic evolution
601 of duplication/loss events compared to other birds (Minias et al., 2019). Here, we used the two
602 copies of MHC gene I and II currently annotated in the collared flycatcher genome as target
603 sequences for our targeted-capture sequencing. The future improvement of genome assembly,
604 thanks to the development of long-reads technology (Peona et al., 2021, 2018), will certainly
605 help to precisely annotate all MHC copies and to study the whole repertoire of MHC genes.

606 *Consequences of drift effect and selection on immunity*

607 The potential relaxation of the natural selection acting on immune genes in island species is
608 expected to reduce immune functions and increase susceptibility of island populations to
609 pathogens. This is true even if this relaxation is only the consequence of a reduction in the
610 effective population size and not caused by a reduction of the pressure exerted by the parasitic
611 community. This is in line with the results of Hawley et al. (2005) and Belasen et al. (2019)
612 who showed that a decrease in diversity of immune loci (MHC II or through immune proxy)
613 was associated with a reduction in immune functions. It should be noted that even if migration
614 rate is reduced on islands, sedentary and endemic island species are not completely free from
615 the exposure of exogen pathogens through migratory birds (Levin et al., 2013).

616 As a final remark, we would like to stress that more research is still needed (i) to ascertain both
617 selection pressures on innate and adaptive immune responses and the load of deleterious
618 mutations due to drift, also identified by an increasing body of work (Loire et al., 2013;
619 Robinson et al., 2016; Rogers and Slatkin, 2017; Kutschera et al., 2020; Leroy et al., 2021b),
620 and (ii) to describe island parasite communities. To date, most of the studies investigated
621 intracellular parasite communities on islands, and more specifically haemosporidian parasites,
622 avian pox and coccidian parasites (Cornuault et al., 2012; Illera et al., 2015, 2008; Ishtiaq et

623 al., 2010; Loiseau et al., 2017; Martinez et al., 2015; Padilla et al., 2017; Pérez-Rodríguez et
624 al., 2013; Silva-Iturriza et al., 2012), whereas very few evaluated the extracellular parasite
625 diversity, such as helminths (Nieberding et al., 2006) but see the review of Illera and Perera
626 (2020) for reptiles. Metabarcoding of parasites is a new technique to evaluate at the same time
627 both communities of intracellular and extracellular parasites (Bourret et al., 2021) and might
628 therefore be a promising approach to evaluate their communities in island and mainland
629 populations.

630 *Conclusion*

631 Our comparative population genomics study has investigated the combined effects of drift and
632 selection on immune genes from island and mainland passerines. The study of synonymous
633 and non-synonymous polymorphism of these genes confirmed that island species, with smaller
634 population sizes than their mainland counterparts, were more impacted by drift, which induces
635 a load of weakly deleterious mutations in their genome. Indeed most of the genes studied here
636 involved in the immune response do not show a statistically different pattern from control
637 genes. Only MHC II genes, involved in the recognition of extracellular pathogens, showed a
638 reduction in their non-synonymous polymorphism in island species. This response, which may
639 be attributed to reduced selection pressures on these genes, could be associated with the
640 suspected reduced parasitic communities on islands. The increased load of deleterious
641 mutations as well as the potential relaxed selection pressures on MHC II support the reduced
642 immune functions of island species, which could be added to the list of other convergent
643 responses of the island syndrome.

644 *Data availability*

645 Datasets, scripts, supplementary figures and texts are available on figshare :
646 https://figshare.com/s/ab7004cc2f4415b4058f. The reads newly generated for this study have
647 been deposited in the NCBI Sequence Read Archive under the bioproject PRJNA724656.

648 *Acknowledgments*

649 In Gabon, we thank the Director and the guides of the Lekedi Park, Marie Charpentier for her
650 help in organizing the expedition, and Alexandre Vaz for field assistance and outreach work.
651 In São Tomé and Príncipe, we thank the Directorate of the Environment and the Department
652 for Nature Conservation, its directors—Arlindo Carvalho and Victor Bonfim—Guilhermino,
653 the Association Monte Pico, its president Luis Mário, and its members. Philippe Perret, Octávio

Veiga, Bikegila, and Yelli provided invaluable assistance in the field. Permissions for fieldwork were given by the authorities of São Tomé and Príncipe and Gabon (CENAREST authorization No. AR0053/12/MENESTFPRSCJS/ CENAREST/CG/CST/CSAR). Permits for the Canary Islands were provided by the Regional Government (Ref.: 2012/0710), and the Cabildo of La Palma and Tenerife. In Montpellier, we thank the blue tit team (https://oreme.org/observation/ecopop/mesanges/) for the capture of the individuals used in this study. The analyses benefited from the Montpellier Bioinformatics Biodiversity (MBB) platform services. This research was conducted in the scope of the international twin-lab "LIA – Biodiversity and Evolution" between CIBIO (Portugal) and ISEM and CEFE-CNRS (France).

Funding information

This research was funded by the Labex CeMEB (project ISLAND IMMUNITY) for BN, the ANR (BirdIslandGenomic project, ANR-14-CE02-0002) for MB, BN, CL and CD, the National Geographic Society (Grant/Award Number:W251-12), the British Ecological Society (Grant/Award Number: 369/4558), the portuguese Foundation for Science and Technology under the PTDC/BIA-EVL/29390/2017 "DEEP" Research Project for MM, RC and CL and the Spanish Ministry of Science, Innovation and Universities, and the European Regional Development Fund (Ref.: PGC2018-097575-B-I00) for JCI.

References

Agudo, R., Alcaide, M., Rico, C., Lemus, J.A., Blanco, G., Hiraldo, F., Donázar, J.A., 2011. Major histocompatibility complex variation in insular populations of the Egyptian vulture: inferences about the roles of genetic drift and selection. Mol. Ecol. 20, 2329–2340. https://doi.org/10.1111/j.1365-294X.2011.05107.x

Akira, S., 2003. Toll-like receptor signaling. J Biol Chem 278, 38105–38108.

Alberts, B., Johnson, A., Lewis, J., Raff, M., Roberts, K., Walter, P., 2002. Innate immunity. Mol. Biol. Cell.

Aphalo, P.J., 2020. ggpmisc: Miscellaneous Extensions to "ggplot2"(R package version 0.3. 6.

Baeckens, S., Van Damme, R., 2020. The island syndrome. Curr. Biol. 30, R338–R339.

Bates, D.M., Maechler, M., Bolker, B., Walker, S., 2012. Package 'lme4.' CRAN R Found Stat Comput.

Beadell, J.S., Atkins, C., Cashion, E., Jonker, M., Fleischer, R.C., 2007. Immunological change in a parasite-impoverished environment: divergent signals from four island taxa. PLoS One 2:e896.

Beadell, J.S., Ishtiaq, F., Covas, R., Melo, M., Warren, B.H., Atkinson, C.T., Bensch, S., Graves, G.R., Jhala, Y.V., Peirce, M.A., 2006. Global phylogeographic limits of Hawaii's avian malaria. Proc R Soc Lond B Biol Sci 273, 2935–2944.

Belasen, A.M., Bletz, M.C., S, L.D., Toledo, L.F., James, T.Y., 2019. Long-term habitat

692 fragmentation is associated with reduced MHC IIB diversity and increased infections
693 in amphibian hosts. Front Ecol Evol 6.
694 Bernatchez, L., Landry, C., 2003. MHC studies in nonmodel vertebrates: what have we
695 learned about natural selection in 15 years? J Evol Biol 16, 363–377.
696 Bjorkman, P.J., Parham, P., 1990. Structure, function, and diversity of class I major
697 histocompatibility complex molecules. Annu Rev Biochem 59, 253–288.
698 Blondel, J., 2000. Evolution and ecology of birds on islands: trends and prospects. Vie
699 MilieuLife Environ. 205–220.
700 Bourret, V., Gutiérrez López, R., Melo, M., Loiseau, C., 2021. Metabarcoding options to
701 study eukaryotic endoparasites of birds. Ecol. Evol. 11, 10821–10833.
702 Boyce, M.S., 1984. Restitution of gamma-and k-selection as a model of density-dependent
703 natural selection. Annu Rev Ecol Syst 15, 427–447.
704 Breuer, K., Foroushani, A.K., Laird, M.R., Chen, C., Sribnaia, A., Lo, R., Winsor, G.L.,
705 Hancock, R.E., Brinkman, F.S., Lynn, D.J., 2013. InnateDB: systems biology of
706 innate immunity and beyond—recent updates and continuing curation. Nucleic Acids
707 Res 41:D1228–D1233.
708 Buffalo, V., 2021. Quantifying the relationship between genetic diversity and population size
709 suggests natural selection cannot explain Lewontin's paradox. eLife 10, e67509.
710 https://doi.org/10.7554/eLife.67509
711 Castellano, D., James, J., Eyre-Walker, A., 2018. Nearly neutral evolution across the
712 Drosophila melanogaster genome. Mol. Biol. Evol. 35, 2685–2694.
713 Chapman, H., JR, O, H., AS, K., RH, C., RL, W., J., 2016. The evolution of innate immune
714 genes: purifying and balancing selection on β-defensins in waterfowl. Mol Biol Evol
715 33, 3075–3087.
716 Charlesworth, J., Eyre-Walker, A., 2008. The McDonald–Kreitman test and slightly
717 deleterious mutations. Mol Biol Evol 25, 1007–1015.
718 Chen, J., Glémin, S., Lascoux, M., 2020. From drift to draft: how much do beneficial
719 mutations actually contribute to predictions of Ohta's slightly deleterious model of
720 molecular evolution? Genetics 214, 1005–1018.
721 Chen, S., Zhou, Y., Chen, Y., Gu, J., 2018. fastp: an ultra-fast all-in-one FASTQ
722 preprocessor. Bioinformatics 34:i884–i890.
723 Corcoran, P., Gossmann, T.I., Barton, H.J., Slate, J., Zeng, K., 2017. Determinants of the
724 Efficacy of Natural Selection on Coding and Noncoding Variability in Two Passerine
725 Species. Genome Biol. Evol. 9, 2987–3007. https://doi.org/10.1093/gbe/evx213
726 Cornuault, J., Bataillard, A., Warren, B.H., Lootvoet, A., Mirleau, P., Duval, T., Milá, B.,
727 Thébaud, C., Heeb, P., 2012. The role of immigration and in-situ radiation in
728 explaining blood parasite assemblages in an island bird clade. Mol. Ecol. 21, 1438–
729 1452.
730 Covas, R., 2012. Evolution of reproductive life histories in island birds worldwide. Proc R
731 Soc B Biol Sci 279, 1531–1537.
732 Doherty, P.C., Zinkernagel, R.M., 1975. Enhanced immunological surveillance in mice
733 heterozygous at the H-2 gene complex. Nature 256, 50–52.
734 Doutrelant, C., Paquet, M., Renoult, J.P., Grégoire, A., Crochet, P.-A., Covas, R., 2016.
735 Worldwide patterns of bird colouration on islands. Ecol Lett 19, 537–545.
736 Drummond, D.A., Bloom, J.D., Adami, C., Wilke, C.O., Arnold, F.H., 2005. Why highly
737 expressed proteins evolve slowly. Proc. Natl. Acad. Sci. 102, 14338–14343.
738 Drummond, D.A., Wilke, C.O., 2008. Mistranslation-induced protein misfolding as a
739 dominant constraint on coding-sequence evolution. Cell 134, 341–352.
740 Ellegren, H., Smeds, L., Burri, R., Olason, P.I., Backström, N., Kawakami, T., Künstner, A.,
741 Mäkinen, H., Nadachowska-Brzyska, K., Qvarnström, A., 2012. The genomic

742 landscape of species divergence in Ficedula flycatchers. Nature 491, 756–760.
743 Enard, D., Cai, L., Gwennap, C., Petrov, D.A., 2016. Viruses are a dominant driver of protein
744 adaptation in mammals. elife 5, e12469.
745 Eyre-Walker, A., Keightley, P.D., 2007. The distribution of fitness effects of new mutations.
746 Nat. Rev. Genet. 8, 610–618.
747 Fijarczyk, A., Dudek, K., Babik, W., 2016. Selective Landscapes in newt Immune Genes
748 Inferred from Patterns of Nucleotide Variation. Genome Biol Evol 8, 3417–3432.
749 Frankham, R., 1997. Do island populations have less genetic variation than mainland
750 populations? Heredity 78, 311–327.
751 Fu, L., Niu, B., Zhu, Z., Wu, S., Li, W., 2012. CD-HIT: accelerated for clustering the next-
752 generation sequencing data. Bioinformatics 28, 3150–3152.
753 Garamszegi, L.Z., 2006. The evolution of virulence and host specialization in malaria
754 parasites of primates. Ecol Lett 9, 933–940.
755 Garrison, E., Marth, G., 2012. Haplotype-based variant detection from short-read sequencing.
756 Gonzalez-Quevedo, C., Phillips, K.P., Spurgin, L.G., Richardson, D.S., 2015a. 454 screening
757 of individual MHC variation in an endemic island passerine. Immunogenetics 67,
758 149–162. https://doi.org/10.1007/s00251-014-0822-1
759 Gonzalez-Quevedo, C., Spurgin, L.G., Illera, J.C., Richardson, D.S., 2015b. Drift, not
760 selection, shapes toll-like receptor variation among oceanic island populations. Mol.
761 Ecol. 24, 5852–5863.
762 Grant, P.R., 1965. The adaptive significance of some size trends in island birds. 355–367,
763 Evolution.
764 Grueber, C.E., Wallis, G.P., Jamieson, I.G., 2014. Episodic positive selection in the evolution
765 of avian toll-like receptor innate immunity genes. PloS One 9, e89632.
766 Grueber, C.E., Wallis, G.P., Jamieson, I.G., 2013. Genetic drift outweighs natural selection at
767 toll-like receptor (TLR) immunity loci in a re-introduced population of a threatened
768 species. Mol. Ecol. 22, 4470–4482.
769 Guéguen, L., Gaillard, S., Boussau, B., Gouy, M., Groussin, M., Rochette, N.C., Bigot, T.,
770 Fournier, D., Pouyet, F., Cahais, V., Bernard, A., Scornavacca, C., Nabholz, B.,
771 Haudry, A., Dachary, L., Galtier, N., Belkhir, K., Dutheil, J.Y., 2013. Bio++:
772 Efficient Extensible Libraries and Tools for Computational Molecular Evolution.
773 Mol. Biol. Evol. 30, 1745–1750. https://doi.org/10.1093/molbev/mst097
774 Hale, K.A., Briskie, J.V., 2007. Decreased immunocompetence in a severely bottlenecked
775 population of an endemic New Zealand bird. Anim. Conserv. 10, 2–10.
776 Haller, B.C., Messer, P.W., 2017. SLiM 2: Flexible, interactive forward genetic simulations.
777 Mol Biol Evol 34, 230–240.
778 Hawley, D.M., Sydenstricker, K.V., Kollias, G.V., Dhondt, A.A., 2005. Genetic diversity
779 predicts pathogen resistance and cell-mediated immunocompetence in house finches.
780 Biol Lett 1, 326–329.
781 Hill, A.V., 1991. HLA associations with malaria in Africa: some implications for MHC
782 evolution, in: Molecular Evolution of the Major Histocompatibility Complex.
783 Springer, pp. 403–420.
784 Hochberg, M.E., Møller, A.P., 2001. Insularity and adaptation in coupled victim–enemy
785 associations. J Evol Biol 14, 539–551.
786 Illera, J.C., Emerson, B.C., Richardson, D.S., 2008. Genetic characterization, distribution and
787 prevalence of avian pox and avian malaria in the Berthelot's pipit (Anthus berthelotii)
788 in Macaronesia. Parasitol Res 103, 1435–1443.
789 Illera, J.C., Fernández-Álvarez, Á., Hernández-Flores, C.N., Foronda, P., 2015. Unforeseen
790 biogeographical patterns in a multiple parasite system in Macaronesia. J. Biogeogr.
791 42, 1858–1870.

Illera, J.C., Perera, A., 2020. Where are we in the host-parasite relationships of native land vertebrates in Macaronesia? Ecosistemas.

Institute, B., 2019. “Picard Toolkit”, Broad institute, GitHub repository. Picard Toolkit.

Ishtiaq, F., Clegg, S.M., Phillimore, A.B., Black, R.A., Owens, I.P., Sheldon, B.C., 2010. Biogeographical patterns of blood parasite lineage diversity in avian hosts from southern Melanesian islands. J. Biogeogr. 37, 120–132.

Jombart, T., Ahmed, I., 2011. adegenet 1.3-1: new tools for the analysis of genome-wide SNP data. Bioinformatics 27, 3070–3071.

Kappes, D., Strominger, J.L., 1988. Human class II major histocompatibility complex genes and proteins. Annu Rev Biochem 57, 991–1028.

Kassambara, A., 2018. ggpubr:“ggplot2” based publication ready plots. R Package Version 01, 7.

Kimura, M., 1962. On the Probability of Fixation of Mutant Genes in a Population. Genetics 47, 713–719.

Klein, J., 1986. Natural history of the major histocompatibility complex. Wiley.

Kloch, A., Wenzel, M.A., Laetsch, D.R., Michalski, O., Bajer, A., Behnke, J.M., Welc-Falęciak, R., Piertney, S.B., 2018. Signatures of balancing selection in toll-like receptor (TLRs) genes–novel insights from a free-living rodent. Sci. Rep. 8, 1–10.

Kutschera, V.E., Poelstra, J.W., Botero-Castro, F., Dussex, N., Gemmell, N., Hunt, G.R., Ritchie, M.G., Rutz, C., Wiberg, R.A.W., Wolf, J.B.W., 2020. Purifying Selection in Corvids Is Less Efficient on Islands. Mol. Biol. Evol. https://doi.org/10.1093/molbev/msz233

Kuznetsova, A., Brockhoff, P.B., Christensen, R.H., 2017. lmerTest package: tests in linear mixed effects models. J Stat Softw 82, 1–26.

Laine, V.N., Gossmann, T.I., Schachtschneider, K.M., Garroway, C.J., Madsen, O., Verhoeven, K.J., De Jager, V., Megens, H.-J., Warren, W.C., Minx, P., 2016. Evolutionary signals of selection on cognition from the great tit genome and methylome. Nat. Commun. 7, 1–9.

Lamichhaney, S., Berglund, J., Almén, M.S., Maqbool, K., Grabherr, M., Martinez-Barrio, A., Promerová, M., Rubin, C.-J., Wang, C., Zamani, N., 2015. Evolution of Darwin/’s finches and their beaks revealed by genome sequencing. Nature 518, 371–375.

Lee, J.W., Beebe, K., Nangle, L.A., Jang, J., Longo-Guess, C.M., Cook, S.A., Davisson, M.T., Sundberg, J.P., Schimmel, P., Ackerman, S.L., 2006. Editing-defective tRNA synthetase causes protein misfolding and neurodegeneration. Nature 443, 50–55. https://doi.org/10.1038/nature05096

Lee, K.A., 2006. Linking immune defenses and life history at the levels of the individual and the species. Integr Comp Biol 46, 1000–1015.

Leroy, T., Anselmetti, Y., Tilak, M.-K., Bérard, S., Csukonyi, L., Gabrielli, M., Scornavacca, C., Milá, B., Thébaud, C., Nabholz, B., 2021a. A bird’s white-eye view on avian sex chromosome evolution. Peer Community J. 1.

Leroy, T., Rousselle, M., Tilak, M.-K., Caizergues, A.E., Scornavacca, C., Recuerda, M., Fuchs, J., Illera, J.C., De Swardt, D.H., Blanco, G., 2021b. Island songbirds as windows into evolution in small populations. Curr. Biol. 31, 1303-1310. e4.

Levin, I.I., Zwiers, P., Deem, S.L., Geest, E.A., Higashiguchi, J.M., Iezhova, T.A., Jiménez-Uzcátegui, G., Kim, D.H., Morton, J.P., Perlut, N.G., Renfrew, R.B., Sari, E.H.R., Valkiunas, G., Parker, P.G., 2013. Multiple Lineages of Avian Malaria Parasites (Plasmodium) in the Galapagos Islands and Evidence for Arrival via Migratory Birds. Conserv. Biol. 27, 1366–1377. https://doi.org/10.1111/cobi.12127

Levy, H., Fiddaman, S.R., Vianna, J.A., Noll, D., Clucas, G.V., Sidhu, J.K., Polito, M.J., Bost, C.A., Phillips, R.A., Crofts, S., 2020. Evidence of pathogen-induced

immunogenetic selection across the large geographic range of a wild seabird. Mol. Biol. Evol. 37, 1708–1726.
Li, H., 2013. Aligning sequence reads, clone sequences and assembly contigs with BWA-MEM. ArXiv Prepr. ArXiv13033997.
Li, H., Handsaker, B., Wysoker, A., Fennell, T., Ruan, J., Homer, N., Marth, G., Abecasis, G., Durbin, R., 2009. The Sequence Alignment/Map format and SAMtools. Bioinforma Oxf Engl 25, 2078–2079.
Lindström, K.M., Foufopoulos, J., Pärn, H., Wikelski, M., 2004. Immunological investments reflect parasite abundance in island populations of Darwin's finches. Proc R Soc Lond B Biol Sci 271, 1513–1519.
Lobato, E., Doutrelant, C., Melo, M., Reis, S., Covas, R., 2017. Insularity effects on bird immune parameters: A comparison between island and mainland populations in West Africa. Ecol. Evol. 7, 3645–3656.
Loire, E., Chiari, Y., Bernard, A., Cahais, V., Romiguier, J., Nabholz, B., Lourenço, J.M., Galtier, N., 2013. Population genomics of the endangered giant Galapagos tortoise. Genome Biol. 14, R136. https://doi.org/10.1186/gb-2013-14-12-r136
Loiseau, C., Melo, M., Lobato, E., Beadell, J.S., Fleischer, R.C., Reis, S., Doutrelant, C., Covas, R., 2017. Insularity effects on the assemblage of the blood parasite community of the birds from the Gulf of Guinea. J. Biogeogr. 44, 2607–2617.
Lomolino, M.V., 2005. Body size evolution in insular vertebrates: generality of the island rule. J. Biogeogr. 32, 1683–1699. https://doi.org/10.1111/j.1365-2699.2005.01314.x
Losos, J.B., Ricklefs, R.E., 2009. Adaptation and diversification on islands. Nature 457, 830–836.
Lundberg, M., Liedvogel, M., Larson, K., Sigeman, H., Grahn, M., Wright, A., Åkesson, S., Bensch, S., 2017. Genetic differences between willow warbler migratory phenotypes are few and cluster in large haplotype blocks. Evol Lett 1, 155–168.
Luo, R., Liu, B., Xie, Y., Li, Z., Huang, W., Yuan, J., He, G., Chen, Y., Pan, Q., Liu, Y., 2012. SOAPdenovo2: an empirically improved memory-efficient short-read de novo assembler. Gigascience 1.
MacArthur, R.H., Wilson, E.O., 1967. The theory of island biogeography, in: The Theory of Island Biogeography. Princeton university press.
Maria, L., Svensson, E., Ricklefs, R.E., 2009. Low diversity and high intra-island variation in prevalence of avian Haemoproteus parasites on Barbados, Lesser Antilles. Parasitology 136, 1121–1131.
Martinez, J., Vasquez, R.A., Venegas, C., Merino, S., 2015. Molecular characterisation of haemoparasites in forest birds from Robinson Crusoe Island: is the Austral Thrush a potential threat to endemic birds? Bird Conserv. Int. 25, 139–152.
Matson, K.D., 2006. Are there differences in immune function between continental and insular birds? Proc. Biol. Sci. 273, 2267–2274. https://doi.org/10.1098/rspb.2006.3590
Matson, K.D., Beadell, J.S., 2010. Infection, immunity, and island adaptation in birds.
Minias, P., Pikus, E., Whittingham, L.A., Dunn, P.O., 2019. Evolution of copy number at the MHC varies across the avian tree of life. Genome Biol Evol 11, 17–28.
Mueller, J.C., Kuhl, H., Timmermann, B., Kempenaers, B., 2016. Characterization of the genome and transcriptome of the blue tit Cyanistes caeruleus: polymorphisms, sex-biased expression and selection signals. Mol. Ecol. Resour. 16, 549–561. https://doi.org/10.1111/1755-0998.12450
Munoz-Mérida, A., Viguera, E., Claros, M.G., Trelles, O., Pérez-Pulido, A.J., 2014. Sma3s: a three-step modular annotator for large sequence datasets. DNA Res 21, 341–353.
Nguyen, L.-T., Schmidt, H.A., Haeseler, A., Minh, B.Q., 2014. IQ-TREE: a fast and effective

892 stochastic algorithm for estimating maximum-likelihood phylogenies. Mol Biol Evol
893 32, 268–274.
894 Nieberding, C., Morand, S., Libois, R., Michaux, J., 2006. Parasites and the island syndrome:
895 the colonization of the western Mediterranean islands by Heligmosomoides polygyrus
896 (Dujardin, 1845. J Biogeogr 33, 1212–1222.
897 O'Connor, E.A., Hasselquist, D., Nilsson, J.-Å., Westerdahl, H., Cornwallis, C.K., 2020.
898 Wetter climates select for higher immune gene diversity in resident, but not
899 migratory, songbirds. Proc. R. Soc. B Biol. Sci. 287, 20192675.
900 https://doi.org/10.1098/rspb.2019.2675
901 Ohta, T., 1992. The nearly neutral theory of molecular evolution. Annu Rev Ecol Syst 23,
902 263–286.
903 Ortutay, C., Vihinen, M., 2009. Identification of candidate disease genes by integrating Gene
904 Ontologies and protein-interaction networks: case study of primary
905 immunodeficiencies. Nucleic Acids Res 37, 622–628.
906 Padilla, D.P., Illera, J.C., Gonzalez-Quevedo, C., Villalba, M., Richardson, D.S., 2017.
907 Factors affecting the distribution of haemosporidian parasites within an oceanic
908 island. Int. J. Parasitol. 47, 225–235.
909 Paradis, E., Schliep, K., 2019. ape 5.0: an environment for modern phylogenetics and
910 evolutionary analyses in R. Bioinformatics 35, 526–528.
911 Peona, V., Blom, M.P.K., Xu, L., Burri, R., Sullivan, S., Bunikis, I., Liachko, I., Haryoko, T.,
912 Jønsson, K.A., Zhou, Q., 2021. Identifying the causes and consequences of assembly
913 gaps using a multiplatform genome assembly of a bird-of-paradise. Mol Ecol Resour
914 21, 263–286.
915 Peona, V., Weissensteiner, M.H., Suh, A., 2018. How complete are "complete" genome
916 assemblies?—An avian perspective. Mol Ecol Resour 18, 1188–1195.
917 Pérez-Rodríguez, A., Ramírez, Á., Richardson, D.S., Pérez-Tris, J., 2013. Evolution of
918 parasite island syndromes without long-term host population isolation: Parasite
919 dynamics in Macaronesian blackcaps Sylvia atricapilla. Glob Ecol Biogeogr 22,
920 1272–1281.
921 Pinheiro, J., Bates, D., DebRoy, S., Sarkar, D., Heisterkamp, S., Willigen, B., Maintainer, R.,
922 2017. Package 'nlme. Linear Nonlinear Mix Eff Models Version 3.
923 R Core Team, 2018. R: A language and environment for statistical computing.
924 Rando, J.C., Alcover, J.A., Illera, J.C., 2010. Disentangling Ancient Interactions: A New
925 Extinct Passerine Provides Insights on Character Displacement among Extinct and
926 Extant Island Finches. PLOS ONE 5:e12956.
927 Ranwez, V., Harispe, S., Delsuc, F., Douzery, E.J., 2011. MACSE: Multiple Alignment of
928 Coding SEquences accounting for frameshifts and stop codons. PLoS One 6:e22594.
929 Recuerda, M., Vizueta, J., Cuevas-Caballé, C., Blanco, G., Rozas, J., Milá, B., 2021.
930 Chromosome-level genome assembly of the common chaffinch (Aves: Fringilla
931 coelebs): a valuable resource for evolutionary biology. Genome Biol. Evol. 13,
932 evab034.
933 Robinson, J.A., Ortega-Del Vecchyo, D., Fan, Z., Kim, B.Y., Marsden, C.D., Lohmueller,
934 K.E., Wayne, R.K., 2016. Genomic flatlining in the endangered island fox. Curr Biol
935 26, 1183–1189.
936 Rogers, R.L., Slatkin, M., 2017. Excess of genomic defects in a woolly mammoth on
937 Wrangel island. PLoS Genet 13:e1006601.
938 Rohland, N., Reich, D., 2012. Cost-effective, high-throughput DNA sequencing libraries for
939 multiplexed target capture. Genome Res. 22, 939–946.
940 Rousselle, M., Simion, P., Tilak, M.-K., Figuet, E., Nabholz, B., Galtier, N., 2020. Is
941 adaptation limited by mutation? A timescale-dependent effect of genetic diversity on

the adaptive substitution rate in animals. PLoS Genet. 16, e1008668.
Santonastaso, T., Lighten, J., Oosterhout, C., Jones, K.L., Foufopoulos, J., Anthony, N.M., 2017. The effects of historical fragmentation on major histocompatibility complex class II β and microsatellite variation in the Aegean island reptile, Podarcis erhardii. Ecol Evol 7, 4568–4581.
She, R., Chu, J.S.-C., Uyar, B., Wang, J., Wang, K., Chen, N., 2011. genBlastG: using BLAST searches to build homologous gene models. Bioinforma Oxf Engl 27, 2141–2143.
Shultz, A.J., Sackton, T.B., 2019. Immune genes are hotspots of shared positive selection across birds and mammals. Elife 8, e41815.
Siewert, K.M., Voight, B.F., 2020. BetaScan2: Standardized Statistics to Detect Balancing Selection Utilizing Substitution Data. Genome Biol. Evol. 12, 3873–3877. https://doi.org/10.1093/gbe/evaa013
Silva-Iturriza, A., Ketmaier, V., Tiedemann, R., 2012. Prevalence of avian haemosporidian parasites and their host fidelity in the central Philippine islands. Parasitol. Int. 61, 650–657.
Simion, P., Belkhir, K., François, C., Veyssier, J., Rink, J.C., Manuel, M., Philippe, H., Telford, M.J., 2018. A software tool 'CroCo'detects pervasive cross-species contamination in next generation sequencing data. BMC Biol. 16, 1–9.
Singhal, S., Leffler, E.M., Sannareddy, K., Turner, I., Venn, O., Hooper, D.M., Strand, A.I., Li, Q., Raney, B., Balakrishnan, C.N., 2015. Stable recombination hotspots in birds. Science 350, 928–932.
Slade, R.W., McCallum, H.I., 1992. Overdominant vs. frequency-dependent selection at MHC loci. Genetics 132.
Slowikowski, K., Schep, A., Hughes, S., Lukauskas, S., Irisson, J.-O., Kamvar, Z.N., Ryan, T., Christophe, D., Hiroaki, Y., Gramme, P., 2018. Package ggrepel. Autom Position Non-Overlapping Text Labels ggplot2.
Smeds, L., Qvarnstrom, A., Ellegren, H., 2016. Direct estimate of the rate of germline mutation in a bird. Genome Res. gr-204669.
Spiess, A.-N., Spiess, M.A.-N., 2018. Package 'qpcR, in: Model. Anal. Real-Time PCRdata Httpscran R-Proj. OrgwebpackagesqpcRqpcR Pdf.
Spurgin, L.G., Van Oosterhout, C., Illera, J.C., Bridgett, S., Gharbi, K., Emerson, B.C., Richardson, D.S., 2011. Gene conversion rapidly generates major histocompatibility complex diversity in recently founded bird populations. Mol. Ecol. 20, 5213–5225. https://doi.org/10.1111/j.1365-294X.2011.05367.x
Tange, O., 2018. GNU parallel 2018.
van Dijk, A., Veldhuizen, E.J., Haagsman, H.P., 2008. Avian defensins. Vet. Immunol. Immunopathol. 124, 1–18.
Van Riper III, C., Van Riper, S.G., Goff, M.L., Laird, M., 1986. The epizootiology and ecological significance of malaria in Hawaiian land birds. Ecol. Monogr. 56, 327–344.
Velová, H., Gutowska-Ding, M.W., Burt, D.W., Vinkler, M., 2018. Toll-like receptor evolution in birds: gene duplication, pseudogenization, and diversifying selection. Mol Biol Evol 35, 2170–2184.
Warren, B.H., Simberloff, D., Ricklefs, R.E., Aguilée, R., Condamine, F.L., Gravel, D., Morlon, H., Mouquet, N., Rosindell, J., Casquet, J., 2015. Islands as model systems in ecology and evolution: Prospects fifty years after MacArthur-Wilson. Ecol. Lett. 18, 200–217.
Warren, W.C., Clayton, D.F., Ellegren, H., Arnold, A.P., Hillier, L.W., Künstner, A., Searle, S., White, S., Vilella, A.J., Fairley, S., 2010. The genome of a songbird. Nature 464,

757–762.
Welch, J.J., Eyre-Walker, A., Waxman, D., 2008. Divergence and Polymorphism Under the Nearly Neutral Theory of Molecular Evolution. J. Mol. Evol. 67, 418–426. https://doi.org/10.1007/s00239-008-9146-9
Wickham, H., 2016. ggplot2: Elegant Graphics for Data Analysis.
Wikelski, M., Foufopoulos, J., Vargas, H., Snell, H., 2004. Galápagos birds and diseases: invasive pathogens as threats for island species. Ecol. Soc. 9.
Wolf, J.B.W., Künstner, A., Nam, K., Jakobsson, M., Ellegren, H., 2009. Nonlinear Dynamics of Nonsynonymous (dN) and Synonymous (dS) Substitution Rates Affects Inference of Selection. Genome Biol Evol 1, 308–319.
Zhang, G., Parker, P., Li, B., Li, H., Wang, J., 2012. The genome of Darwin's Finch (Geospiza fortis). https://doi.org/10.5524/100040

Supplementary Text & Figures:

Evolution of immune genes in island birds: reduction in population sizes can explain island syndrome

Mathilde BARTHE, Claire DOUTRELANT, Rita COVAS, Martim MELO,
Juan Carlos ILLERA, Marie-Ka TILAK, Constance COLOMBIER, Thibault LEROY ,
Claire LOISEAU , Benoit NABHOLZ

Supplementary Methods :

Test for contamination

Analyses were performed to identify contaminations between individuals of different species. First, we generate assembly for all individuals using Megahits v.1.2.7 (Li et al. 2015). Next, we use the program CroCo (vers. 1.1; Simion et al. 2018) to identify candidates for cross-species contamination. CroCo identifies a contig from the assembly of the species X as contaminated by the species Y if the reads from the species Y map with a higher relative proportion on the contig than the reads for the species X.

Contamination tests were performed on 3765 combinations of individuals from different species. On average, 3.12% of the contigs were considered as contaminants (Figure S1). The top 20% of the combinations (i.e., a value greater than 3.09% of contaminating contigs ; Figure S1) always involve a pair of species belonging to the same genus. In this case, contamination could be difficult to identify due to the low genetic divergence between species. The remaining 80% showed low percentages of contamination (<5% of scaffolds) that may be associated with false positives (i.e., corresponding to highly conserved sequences between species). Overall, we did not detect a clear case of cross-species contamination in our dataset.

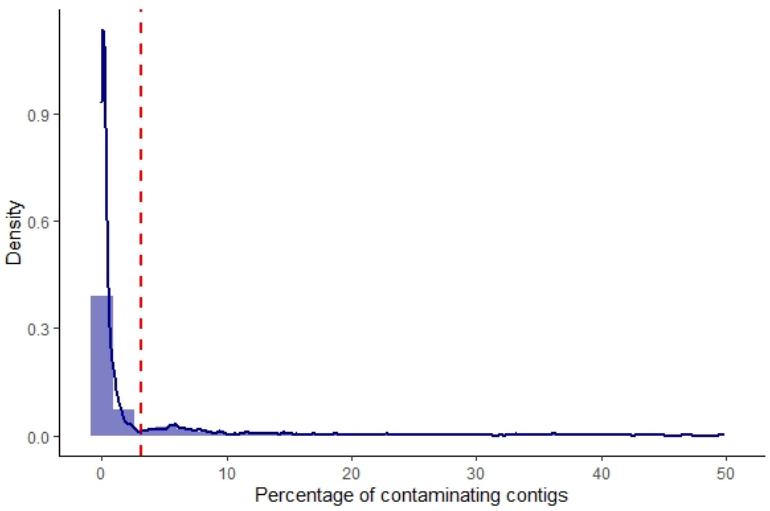

Figure S1: Distribution of the percentage of contaminating contigs. The red line represents the 80% quantile.

Homology identification

After defining the genes composition of our differents group, see Selection and identification of immune and control genes, we obtained their reference sequences from the Ensembl database for core groupe and control group and from the annotated genome of *F. albicolis for* Database groupe and Sma3s groupe. We also used the TLRs alignments from Velová et al. (2018).

Then, in order to identify corresponding sequences in our 11 reference genomes, we search for homologous sequences. To do so, we first translated sequences with transeq (vers. 6.6.0.0; Rice et al. 2000), then we used the program Silix (vers. 1.2.9; Miele et al. 2011) to cluster amino-acid sequences with at least 60% of similarity and a minimum overlap of 30%. For partial sequences, a minimum length of 10 amino acids or a minimum of 5% of the complete protein sequence was required.

For the immunity genes, some sequences could be assigned to several clusters due to paralogy (*e.g.*, TLR2A and TLR2B). In the core group, we use the probabilistic approach of the profile hidden Markov models implemented in HMMER (v. 3.3.2; Mistry et al. 2013) to assign the gene to a cluster. We first created a gene-specific HMM profile from the alignments of Velová et al. (2018). Then, the candidate sequences were assigned to each homologous group based on the best score of a hmmscan search. For larger sets of genes (i.e Database-group and Sma3s-group), we remove duplicated sequences in the dataset to analyse only one.

Detection of genes under balancing selection

The Database-group and Sma3s-group most likely include immune genes subject to different selection pressures (*i.e.*, balancing and purifying selection). To identify genes evolving under balancing selection, unfolded SNP frequency was estimated using a home-made script for *Taeniopygia guttata* using *Poephila acuticauda* as outgroup. The allelic state of *Poephila* was taken as the ancestral state of *Taeniopygia*. Then, we run the program BetaScan (vers. 2; Siewert and Voight 2020) with a sliding window of 2000pb and option '-fold -m 0.15' allowed to exclude allele with a frequency under 15% to avoid false positives to identify SNPs. We selected the top SNPs with a score above a 99.9% threshold based on the Beta* score as evolving under balancing selection (Siewert and Voight 2020). Finally, genes overlapping with the top SNPs were considered as genes evolving under balancing selection or overdominance. Respectively only 2 and 3 genes from Database-group and Sma3s-group sets were identified and removed from the analysis.

Simulation of control genes under balancing selection

Simulations were performed using SLiM software (vers. 3.3.2; Haller and Messer 2017). Sequences of 300kb with a mutation of 4.6e-9 substitutions/site/generation were simulated (Smeds et al. 2016). Recombination was set to be equal to mutation rate. Three types of mutations were possible: i) neutral synonymous mutations, ii) non-synonymous mutations

with a Distribution of Fitness Effect (DFE) following a gamma law of mean = -0.025 and shape = 0.3, which corresponds to the DFE estimated in Passerines by Rousselle et al. (2020), iii) non-synonymous mutations under balancing selection with an effect on fitness initially set at 0.01 but re-estimated by the program at each generation according to the mutation frequency in the population, thus including a frequency-dependent effect.

We simulate a coding sequence organization where positions one and two of the codons were considered as non-degenerated sites with the two non-synonymous types of mutations previously described are possible in proportion of 1 mutation under balancing selection for 6 randomly sampled in the DFE. The third position was considered as a 4-fold degenerate site, where only synonymous mutations could appear.

Two population sizes were simulated. One of 270,000 individuals representing large mainland population sizes, and another of 110,000 individuals representing smaller island populations. These values were estimated from the synonymous nucleotide diversity (Ps) estimated for insular and mainland species in our dataset (see part *Polymorphism analyses* from Materials) which allow the estimation of the effective population size as $Ne = Ps / 4*\mu$ (with μ=4.6e-9 corresponding to mutation rate estimated for the collared flycatcher in Smeds et al. 2016). Simulations were replicated 15 times, by sampling the genome of 15 individuals after 100,000 generations, of which 10,000 generations corresponded to a burning phase. Nucleotide diversity of non-degenerated and 4-fold degenerate sites were estimated by arithmetic averaging the divergences of all sequence pairs (Tajima 1989).

Next, we simulated the effect of population size variation on Pn/Ps under two types of balancing selection, namely frequency-dependence and overdominance (Figure S4, S5). In both cases, we simulated 10 population sizes for both island and mainland populations (starting respectively from 1100 and 2700 individuals and doubled between each population size step), 10 replicas were made for each population size. We use the same parameters as before, except for the non-synonymous mutation, where for i) frequency dependence, mutations were initially set a fitness effect of 0.01 and then re-estimated at each generation according to the mutation frequency in the population, and ii) for overdominance, mutations sets a fitness effect of 0.01 and a dominance coefficient of 1.5.

Finally, we tested the effect of selection coefficient variation. To do so, we fixed population size at 110,000 individuals and made the fitness vary from 0 to 0.045 for frequency dependence mutation (Figure S6A), and the dominance coefficient (h) from 1.0 to 1.8 for overdominance mutations (Figure S6B).

Supplementary figures and tables:

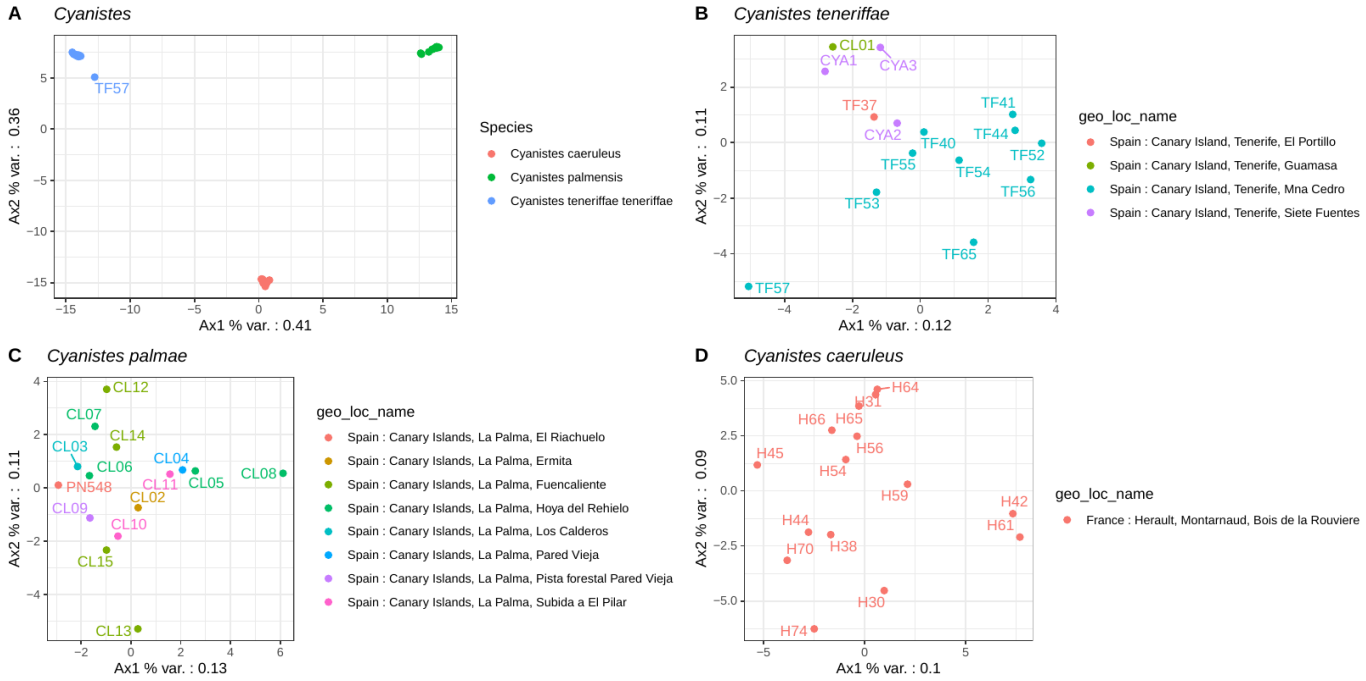

<u>Figure S2</u>: Principal Component Analysis PCA using alleles frequencies of the control genes. A) All *Cyanistes* species; B) *Cyanistes teneriffae*; C) *Cyanistes palmensis*; D) *Cyanistes caeruleus*. Colors indicate species or locality.

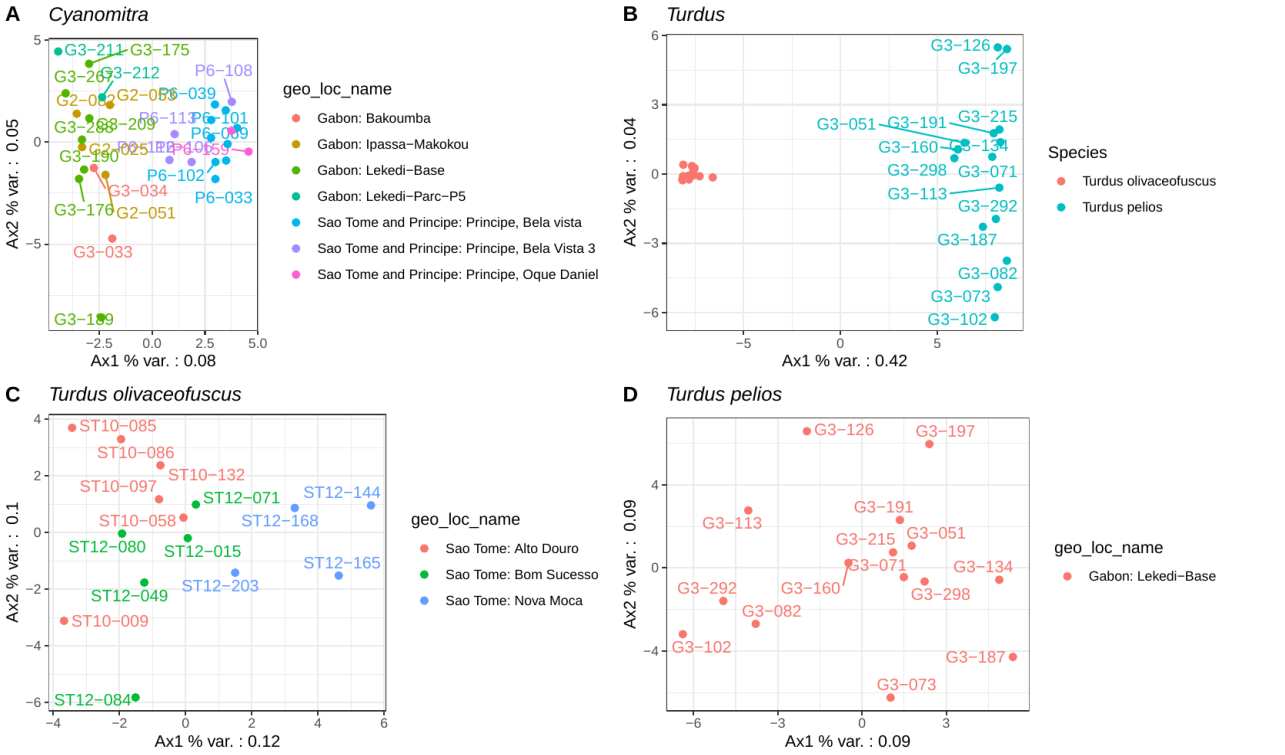

Figure S3: Principal Component Analysis PCA using alleles frequencies of the control genes. A) *Cyanomitra olivacea;* B) All *Turdus* species; C) *Turdus olivaceofuscus*; D) *Turdus pelios*. Colors indicate species or locality.

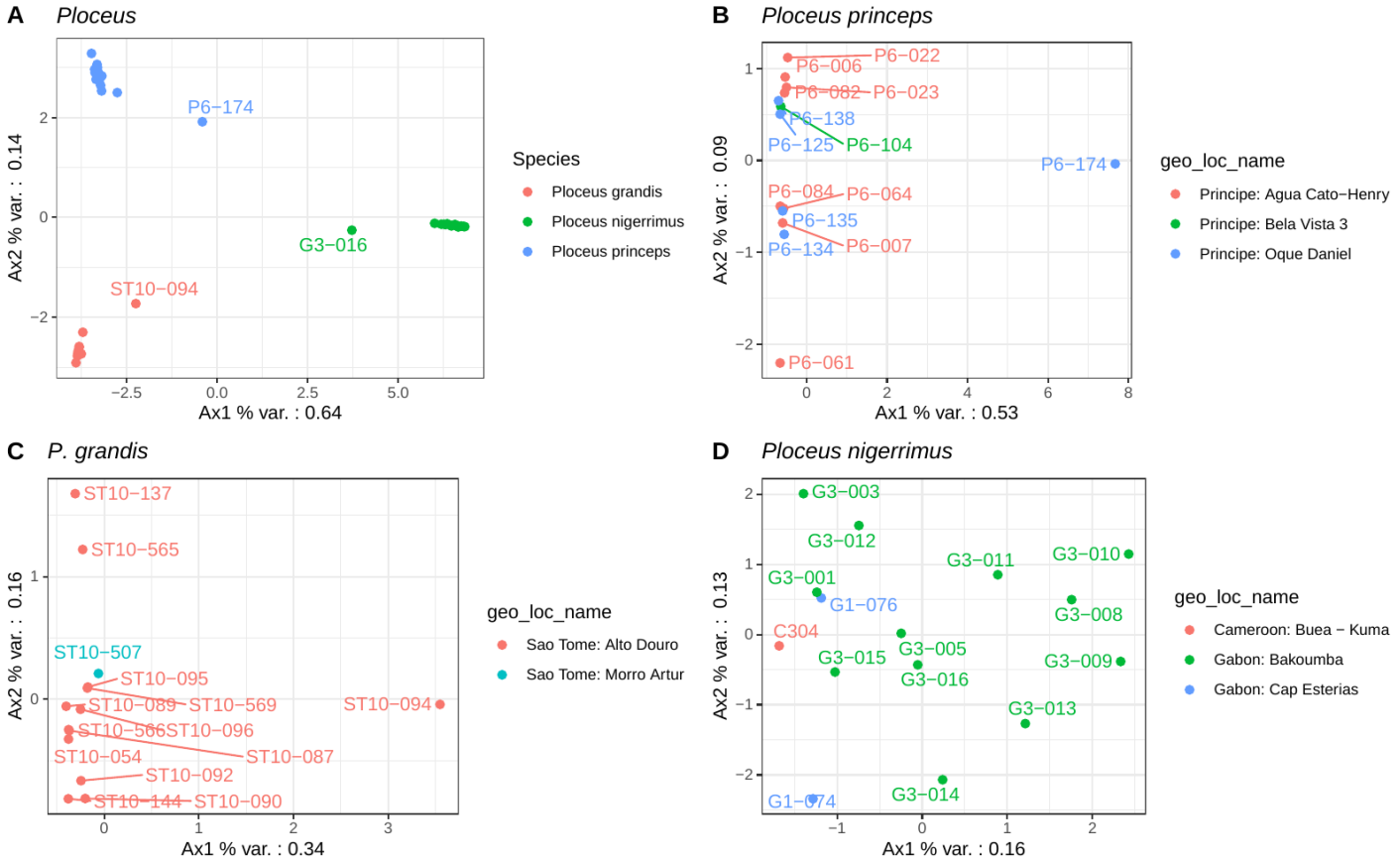

Figure S4: Principal Component Analysis PCA using alleles frequencies of the control genes. A) All *Ploceus* species; B) *Ploceus princeps*; C) *Ploceus grandis*; D) *Ploceus nigerrimus*. Colors indicate species or locality.

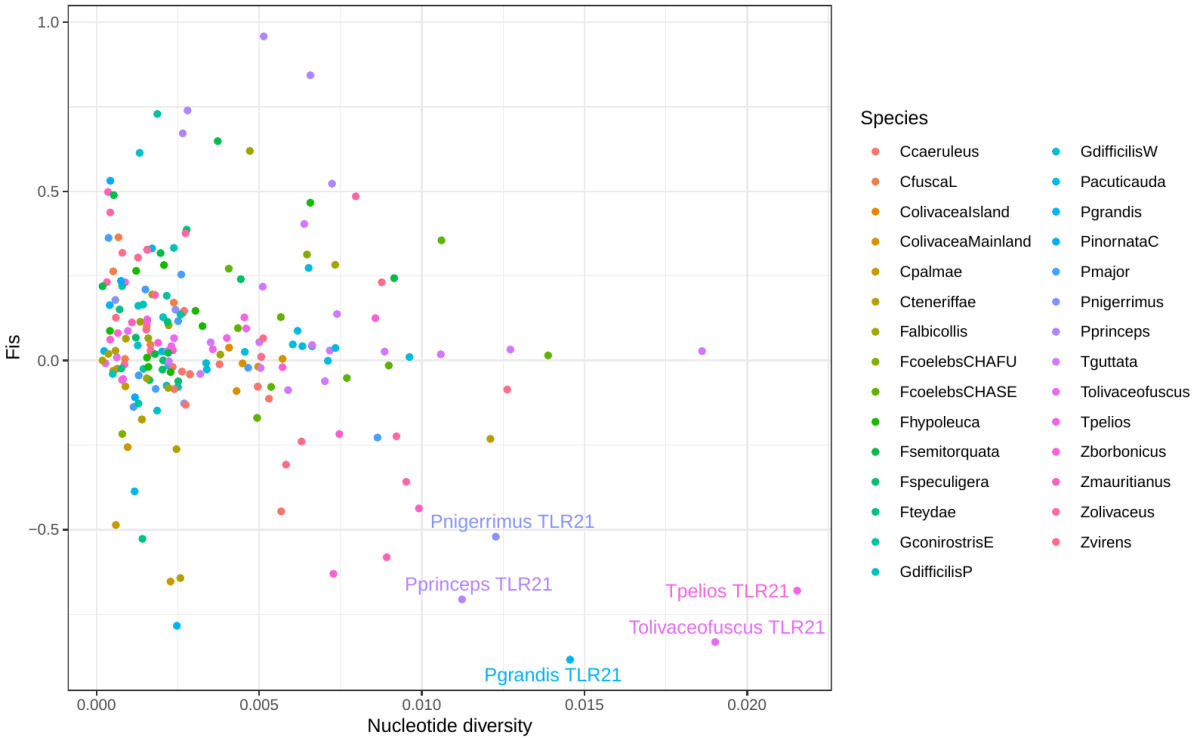

Figure S5: Deviation of heterozygosity from Hardy-Weinberg proportion (Fis) according to nucleotide diversity (Pi). A negative Fis indicates more heterozygous individuals than expected.

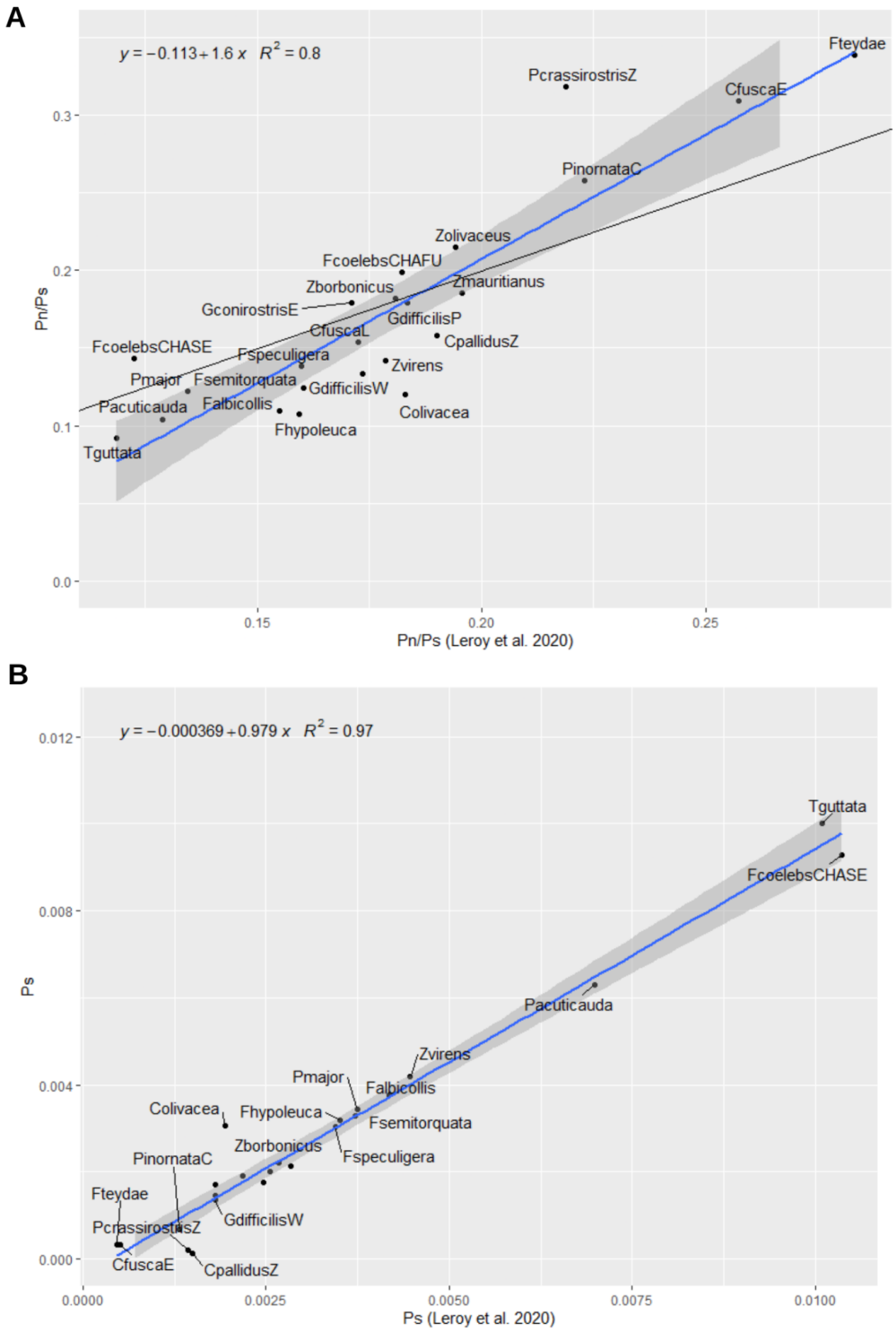

Figure S6: Correlation between Pn/Ps (a) and Ps (b) calculated on the control genes in this study's dataset and those calculated by Leroy et al. (2021). Ps: synonymous polymorphism Pn: non-synonymous polymorphism.

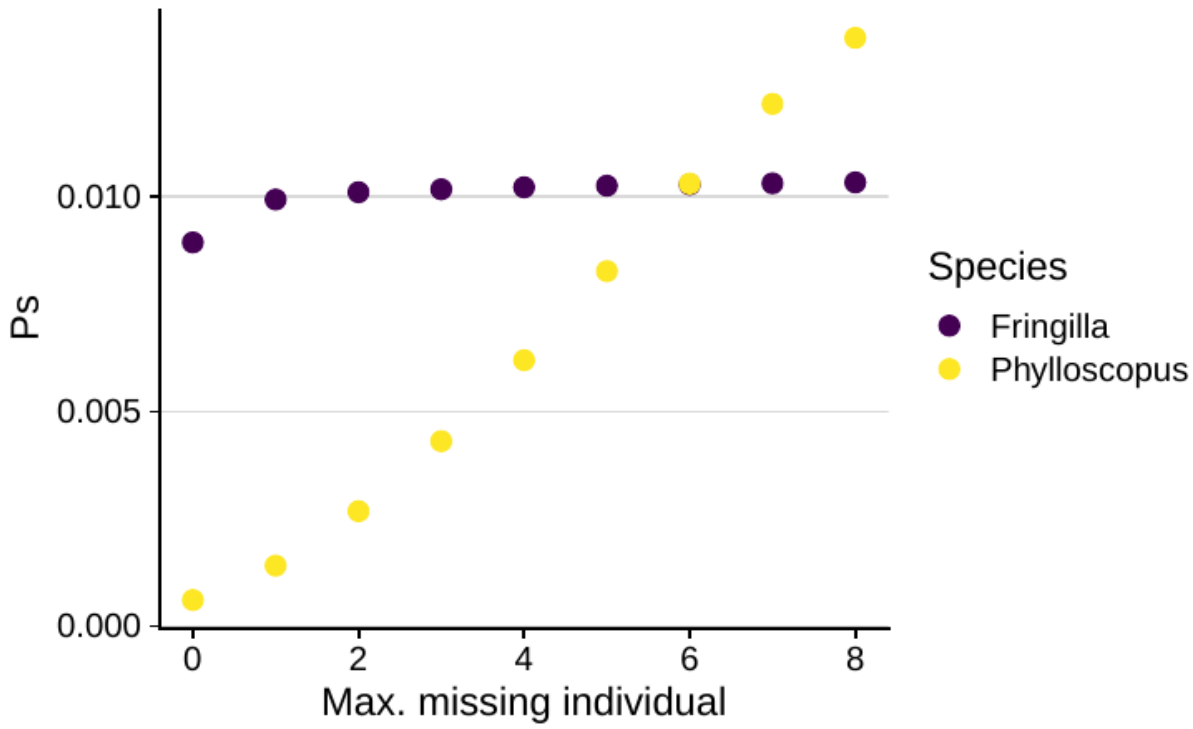

Figure S7: Relationship between the maximum number of missing individuals allowed and synonymous nucleotide diversity (Ps)in *Phylloscopus trochilus* and *Fringilla coelebs*.

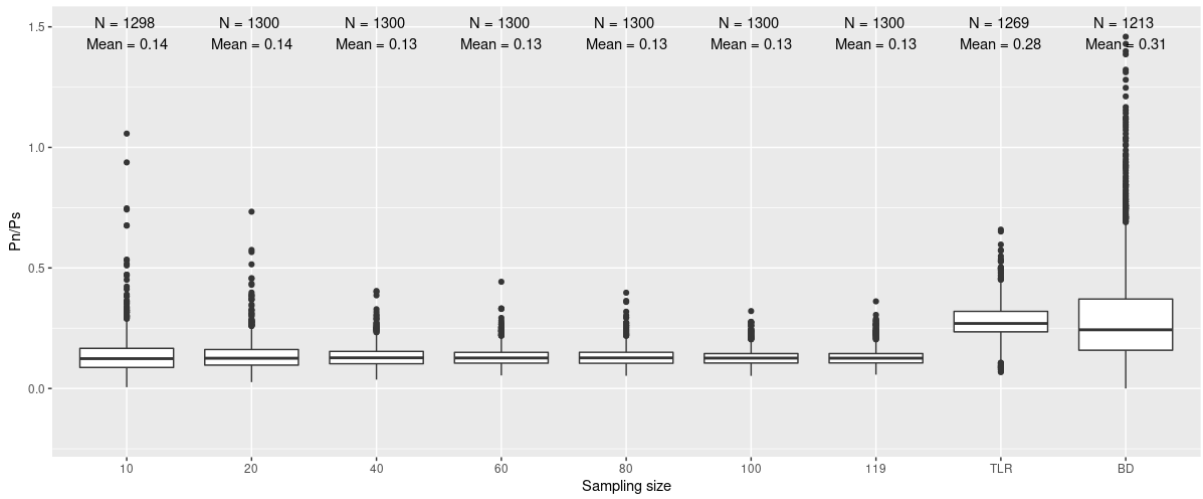

Figure S8: Effect of sub-sampling size on PN/PS. Bootstrap of 100.For BD samplig of 9 genes, for TLR sampling of 10 genes.

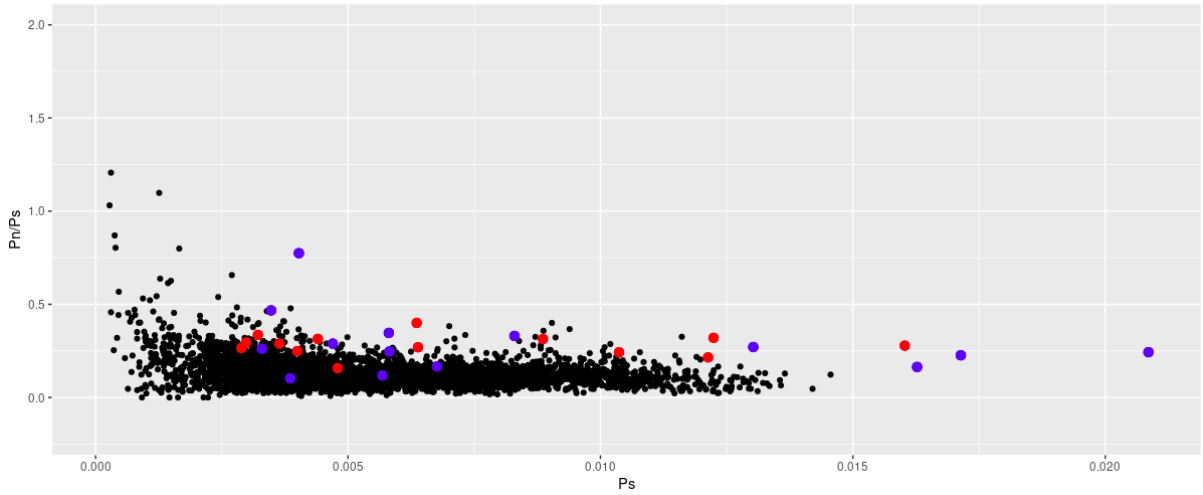

Figure S9: Effect of sub-sampling of control genes, here each point corresponds to the values of a mainland species calculated on 10 randomly selected control genes. In blue the BD, in red the TLR gene.

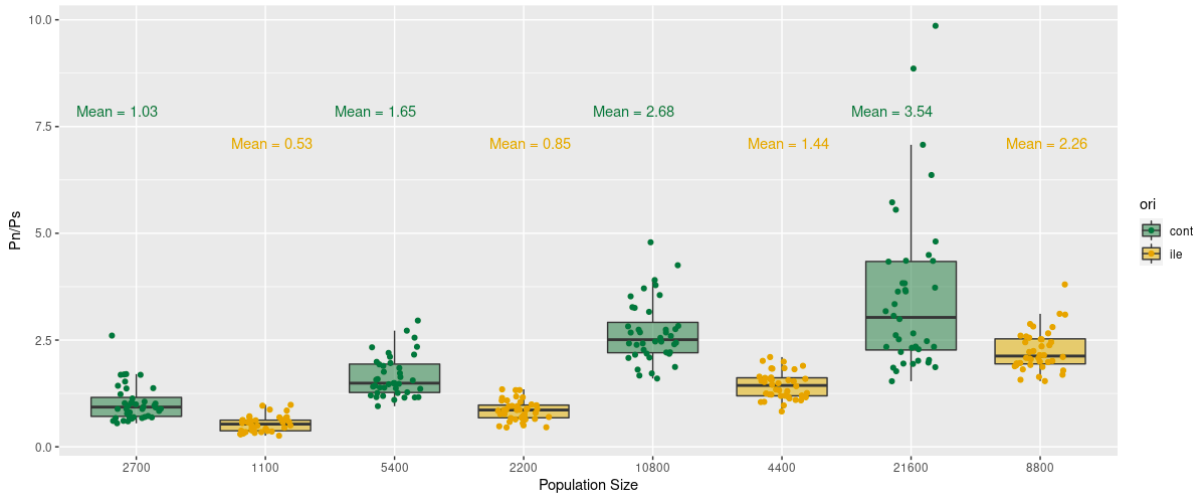

Figure S10: Boxplot of Pn/Ps according to population size for simulated sequences under overdominance with SLiM. Dominance coefficient is fixed at 1.5. Each modality is replicated 10 times.

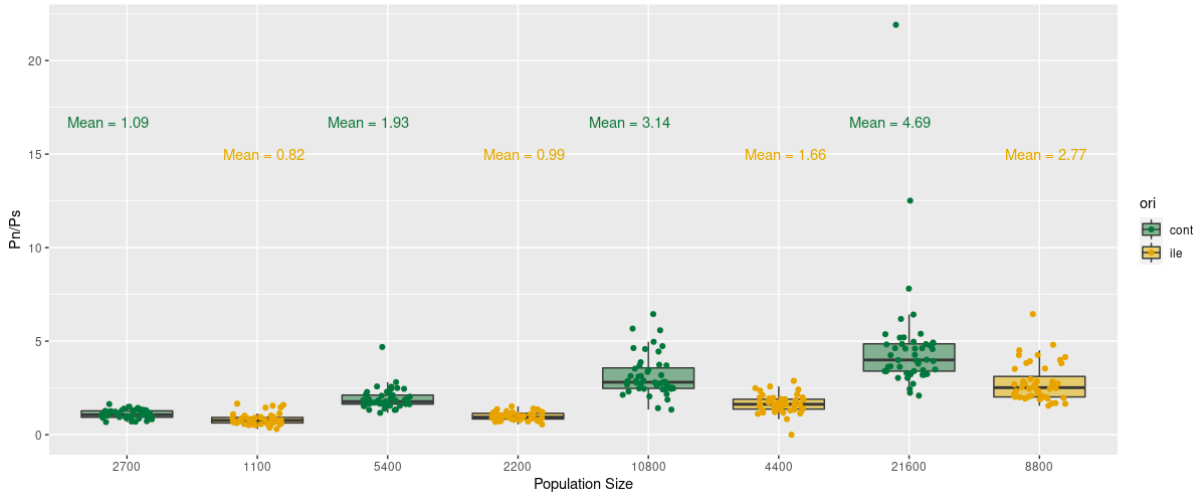

Figure S11: Boxplot of Pn/Ps according to population size for simulated sequences under frequency dependence with SLiM. Each modality is replicated 10 times.

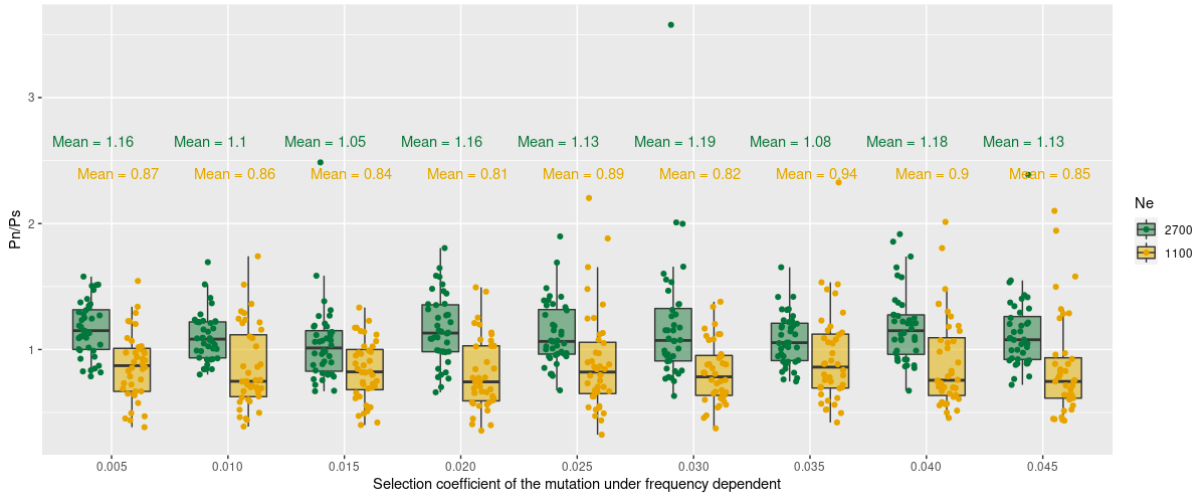

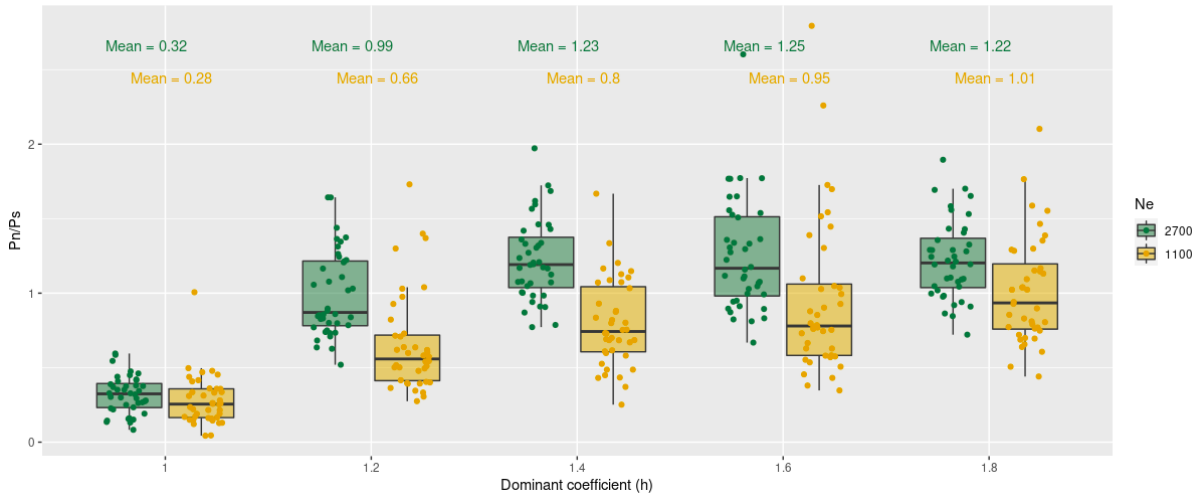

Figure S12: Boxplot of Pn/Ps according to a) initial selection coefficient of the mutation under frequency dependence b) dominance coefficient (h) for simulated sequences under overdominance with SLiM. Each modality is replicated 10 times.

Table S1: Model selection of all gene categories using a reduced number of families (we grouped Turdidae within Muscicapidae, Nectariniidae, and Estrildidae within Ploceidae and Fringillidae within Thraupidae).
https://figshare.com/s/ab7004cc2f4415b4058f

Table S2: Summary of the linear model and PGLS model using phylogeny from Figure 1 and the ΔPn/Ps (difference between the Pn/Ps of immune genes and control genes).
https://figshare.com/s/ab7004cc2f4415b4058f

Table S3: Table with information regarding the samples newly-sequenced in this study.
https://figshare.com/s/ab7004cc2f4415b4058f

Table S4: Table with information regarding the sample obtained from Leroy et al. 2021.
https://figshare.com/s/ab7004cc2f4415b4058f
Table S5 to S14: Model selection by AICc criterion and ANOVA test. Summary of the best models.
https://figshare.com/s/ab7004cc2f4415b4058f
Table S15 to S24:
https://figshare.com/s/ab7004cc2f4415b4058f

References

Haller BC, Messer PW. 2017. SLiM 2: Flexible, interactive forward genetic simulations. *Mol. Biol. Evol.* 34:230–240.

Li D, Liu C-M, Luo R, Sadakane K, Lam T-W. 2015. MEGAHIT: an ultra-fast single-node solution for large and complex metagenomics assembly via succinct de Bruijn graph. *Bioinformatics* 31:1674–1676.

Miele V, Penel S, Duret L. 2011. Ultra-fast sequence clustering from similarity networks with SiLiX. *BMC Bioinformatics* 12:1–9.

Mistry J, Finn RD, Eddy SR, Bateman A, Punta M. 2013. Challenges in homology search: HMMER3 and convergent evolution of coiled-coil regions. *Nucleic Acids Res.* 41:e121–e121.

Rice P, Longden I, Bleasby A. 2000. EMBOSS: the European molecular biology open software suite. *Trends Genet.* 16:276–277.

Rousselle M, Simion P, Tilak M-K, Figuet E, Nabholz B, Galtier N. 2020. Is adaptation limited by mutation? A timescale-dependent effect of genetic diversity on the adaptive substitution rate in animals. *PLoS Genet.* 16:e1008668.

Siewert KM, Voight BF. 2020. BetaScan2: Standardized Statistics to Detect Balancing Selection Utilizing Substitution Data. *Genome Biol. Evol.* 12:3873–3877.

Simion P, Belkhir K, François C, Veyssier J, Rink JC, Manuel M, Philippe H, Telford MJ.

2018. A software tool ‘CroCo’detects pervasive cross-species contamination in next generation sequencing data. *BMC Biol.* 16:1–9.
Smeds L, Qvarnstrom A, Ellegren H. 2016. Direct estimate of the rate of germline mutation in a bird. *Genome Res.*:gr-204669.
Tajima F. 1989. Statistical method for testing the neutral mutation hypothesis by DNA polymorphism. *Genetics* 123:585–595.
Velová H, Gutowska-Ding MW, Burt DW, Vinkler M, Yeager M. 2018. Toll-like receptor evolution in birds: gene duplication, pseudogenisation and diversifying selection. *Mol. Biol. Evol.*